



CHALMERS
UNIVERSITY OF TECHNOLOGY

Molecular imaging mass spectrometry for probing protein dynamics in neurodegenerative disease pathology

Downloaded from: <https://research.chalmers.se>, 2025-12-04 23:29 UTC

Citation for the original published paper (version of record):

Michno, W., Wehrli, P., Blennow, K. et al (2019). Molecular imaging mass spectrometry for probing protein dynamics in neurodegenerative disease pathology. *Journal of Neurochemistry*, 151(4): 488-506. <http://dx.doi.org/10.1111/jnc.14559>

N.B. When citing this work, cite the original published paper.

REVIEW

Molecular imaging mass spectrometry for probing protein dynamics in neurodegenerative disease pathology

Wojciech Michno* , Patrick M. Wehrli*, Kaj Blennow*[†],
Henrik Zetterberg*^{†‡§}  and Jörg Hanrieder*^{‡¶} ^{*}Department of Psychiatry and Neurochemistry, the Sahlgrenska Academy at the University of Gothenburg, Mölndal, Sweden[†]Clinical Neurochemistry Laboratory, Sahlgrenska University Hospital, Mölndal, Sweden[‡]Department of Neurodegenerative Disease, UCL Institute of Neurology, University College London, London, UK[§]UK Dementia Research Institute at UCL, London, UK[¶]Department of Chemistry and Chemical Engineering, Chalmers University of Technology, Gothenburg, Sweden

Abstract

Recent advances in the understanding of basic pathological mechanisms in various neurological diseases depend directly on the development of novel bioanalytical technologies that allow sensitive and specific chemical imaging at high resolution in cells and tissues. Mass spectrometry-based molecular imaging (IMS) has gained increasing popularity in biomedical research for mapping the spatial distribution of molecular species *in situ*. The technology allows for comprehensive, untargeted delineation of *in situ* distribution profiles of metabolites, lipids, peptides and proteins. A major advantage of IMS over conventional histochemical techniques is its superior molecular specificity. Imaging mass spectrometry

has therefore great potential for probing molecular regulations in CNS-derived tissues and cells for understanding neurodegenerative disease mechanism. The goal of this review is to familiarize the reader with the experimental workflow, instrumental developments and methodological challenges as well as to give a concise overview of the major advances and recent developments and applications of IMS-based protein and peptide profiling with particular focus on neurodegenerative diseases.

Keywords: Alzheimer's disease, beta-amyloid, imaging mass spectrometry, matrix-assisted laser desorption/ionization, molecular imaging, neurodegeneration.

J. Neurochem. (2019) **151**, 488–506.

[This article is part of the Special Issue "Proteomics".](#)

Received April 15, 2018; revised manuscript received June 10, 2018, July 3, 2018; accepted July 12, 2018.

Address correspondence and reprint requests to Jörg Hanrieder, Department of Psychiatry and Neurochemistry, Sahlgrenska Academy at the University of Gothenburg, Mölndal Hospital, House V, S-431 80 Mölndal, Sweden. E-mail: jh@gu.se

Abbreviations used: 1,5-DAN, 1,5-diamino naphthalene; 2,5 DHB, 2,5-dihydroxy benzoic acid; 2,5-DHA, 2,5-dihydroxy acetophenone; 6-OHDA, 6-hydroxy-dopamine; AD, Alzheimer's disease; ALS, amyotrophic lateral sclerosis; APOE4, apolipoprotein E; APP, amyloid precursor protein; aSyn, alpha synuclein; A β , beta-amyloid; BMAA, beta-methylamino-L-alanine; ChiP, chemical inkjet printer; DESI, desorption electrospray ionization; ESI, electrospray ionization; FTICR, Fourier transform ion cyclotron resonance; HCA, hierarchical cluster analysis;

HCCA, 4-hydroxy-alpha cyano cinnamic acid; HD, Huntington's disease; Htt, huntingtin; IHC, immunohistochemistry; IMS, imaging mass spectrometry; IP, immunoprecipitation; LC, liquid chromatography; LID, L-DOPA-induced dyskinesia; LPC, lysophosphatidylcholines; MAF, maximum autocorrelation factor analysis; MALDI, matrix-assisted laser desorption/ionization; MIF, macrophage inhibitory factor; MPTP, 1-methyl-4-phenyl-1,2,3,6-tetrahydropyridine; MSc, multiples sclerosis; MS, mass spectrometry; NFM, neurofilament M; NGR, neurogranin; NMF, non-negative matrix factorization; PCA, principal component analysis; PC, posphatidylcholines; PD, Parkinsons disease; PDyn, prodynorphin; PI, phosphoinositol; PLSA, probabilistic latent semantic analysis; ROI, regions of interest; SALDI, surface activated laser desorption/ionization; SA, sinapinic acid; SIMS, secondary ion mass spectrometry; ToF, time of flight; Tyb4, thymosin beta 4; Ubc, ubiquitin.

Background

Many neurodegenerative diseases including Alzheimer's disease (AD), Parkinson's disease (PD), Huntington's disease, Amyotrophic lateral sclerosis (ALS), and multiples sclerosis are characterized by progressive neuronal degeneration and accumulation of misfolded proteins into intra and/or extra cellular neurotoxic deposits (Taylor *et al.* 2002). However, the exact molecular mechanisms that account for neurodegeneration and protein pathology in these diseases are still not resolved, which in turn significantly hampers the development of curative treatment strategies. One factor contributing to the limited understanding of the underlying molecular mechanisms in neurodegenerative diseases is the paucity of biochemical tools that feature the necessary sensitivity, specificity, spatial- and temporal resolution, respectively, in order to delineate molecular mechanisms at cellular length scales. In this respect, chemical imaging techniques are essential bioanalytical tools to gain in-depth understanding of molecular changes at the subcellular level. For probing spatial changes of distinct molecular targets *in vivo* and *in situ*, different biochemical imaging technologies can be employed. This includes primarily immunohistochemistry (IHC) and *in situ* hybridization but also the use of chemical probes (Aslund *et al.* 2009), nanoparticles (Smith and Gambhir 2017), proximity ligation/extension (Gomes *et al.* 2016) as well as spectroscopic methods (Evans *et al.* 2005; Schmid *et al.* 2013). However, a major challenge lies on obtaining suitable spatial resolution while maintaining high molecular specificity and selectivity as well as high sensitivity.

The advent of novel ionization techniques for mass spectrometry that facilitate soft ionization of large biomolecules, including matrix-assisted laser desorption ionization (MALDI) (Karas and Hillenkamp 1988; Tanaka *et al.* 1988) and electrospray ionization (ESI) (Fenn *et al.* 1989) paved the way for mass spectrometry (MS) to become the method of choice for protein and peptide characterization giving rise to an entire novel research field, proteomics (Aebersold and Mann 2003), corresponding to the characterization of all proteins in a biological sample at a distinct condition and place in time. Mass spectrometry-based proteomics of dissected tissues is a valuable tool for sensitive *in situ* identification and quantitation of proteins and endogenous peptides, including, e.g., neuropeptides (Svensson *et al.* 2003). However, a major limitation in tissue proteomics remains with respect to delineating spatial resolution of analyte localization, as spatial information within the respective tissue compartment is not obtained. Given the complexity of the human nervous system, spatial information on protein and peptide distributions is of significant interest in order to resolve ongoing molecular mechanisms. Moreover, neuroactive peptide species are involved in numerous neuronal signaling processes and their localization is, therefore, of essential relevance for

identifying their distinct role in the respective signaling pathways.

Imaging mass spectrometry

Imaging mass spectrometry (IMS) has been demonstrated to be a powerful approach for probing spatial distributions of molecular species *in situ*. Unlike other, more established, biochemical imaging techniques, IMS allows for label-free analysis without any *a priori* knowledge of the potential target species. Although IMS analyses are by nature untargeted, the sample preparation can be tailored for different classes of target molecules of interests. The most prominent IMS techniques include MALDI-based IMS, time of flight secondary ion mass spectrometry (ToF-SIMS) imaging and desorption electrospray ionization IMS (DESI). In MALDI IMS, commonly a UV laser is used for ion desorption and ionization from tissue sections that have been pre-coated with a UV-light absorbing matrix (Spengler *et al.* 1994; Caprioli *et al.* 1997). In ToF-SIMS, molecular species are desorbed and ionized using a focused beam of primary ions (Fletcher *et al.* 2011); while DESI is based on focusing an electrospray onto the sample surface allowing IMS data acquisition at atmospheric pressure (Takats *et al.* 2004).

The different ionization methods employed in IMS are characterized by complementary strengths and limitations, which concerns mainly the spatial resolution, mass accuracy and mass resolution, chemical specificity, selectivity as well as molecular mass range (McDonnell and Heeren 2007).

The common IMS procedure involves the sequential acquisition of mass spectrometry experiments *in situ* in a pre-defined raster pattern or array, termed microprobe mode (Spengler *et al.* 1994) (Fig. 1). Alternatively, efforts have been demonstrated to perform IMS in microscopy mode, where a wide field of view is desorbed by an unfocused projectile following transfer and visualization of the desorbed ions using electromagnetic lenses (Luxembourg *et al.* 2004). Both methods allow then to generate spatial intensity distribution maps of a distinct molecular species over the analyzed mass spectrometry analysis array (Fig. 1c).

For assessing the performance and suitability of IMS for analysis of different molecular species in different tissues and with different biological context, typically two parameters are considered primarily: (i) spatial resolution and (ii) molecular mass range. Both parameters depend on the desorption method including the size of the probe and the mass detector architecture as well as importantly the sample preparation.

Spatial resolution of an IMS method is commonly interchangeably used with pixel resolution, defined by the point-to-point distance of each spot where an MS experiment is acquired according to the pre-defined acquisition pattern. However, this is only true for discontinuous microprobe mode experiment (McDonnell and Heeren 2007). In contrast, continuous IMS methodologies have been presented, where

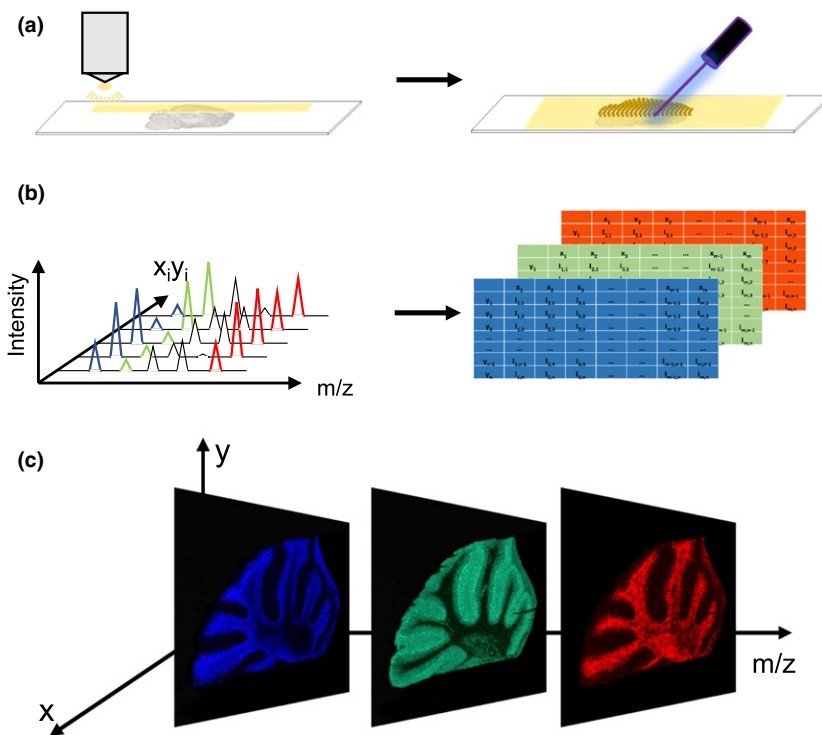


Fig. 1 Principle of imaging mass spectrometry (MALDI-IMS). (a) Tissue sections are collected, mounted on a target for imaging mass spectrometry and, in case of MALDI IMS, pre-coated with a matrix (indicated in yellow), before systematic scanning with a laser probe. (b) One mass spectrum is acquired for every x_j , y_j coordinate of the scanned tissue section. (c) Single ion images are generated by mapping the intensity of an individual ion signal (m/z ;rel.Int) over the whole tissue section.

the probe is continuously sampling while the sample stage is moved at constant speed (Simmons 2008; Spraggins and Caprioli 2011). Moreover, the actual spatial resolution corresponds rather to the size of the probe and the ability to desorb the sample from two adjacent spots without interfering signal. A further special case of microprobe imaging MS, that potentially complicates the definition of spatial resolution, is oversampling, where the pixel resolution is smaller than the size of the probe (Jurchen *et al.* 2005; Wiegmann *et al.* 2016). This illustrates that the resolution terminology as used, e.g., for optical imaging cannot directly be adopted to IMS. For convenience in this review, the term ‘spatial resolution’ will be used hereafter when discussing the lateral resolution of intensity distribution data generated by IMS.

IMS provides high molecular specificity afforded by mass spectrometry, allowing comprehensive image analysis of a multitude of lipids, peptide and proteins in complex biological tissues (for other comprehensive reviews see: Cornett *et al.* 2007; Seeley and Caprioli 2008; McDonnell and Heeren 2007; Norris and Caprioli 2013). Using IMS allows the identification of chemical profiles associated with histological features and regions of interest (ROI). IMS and in particular MALDI IMS have therefore over the last 10–15 years become a more and more recognized technology for probing histochemical changes associated with disease pathology, primarily in cancer research (Schwamborn and Caprioli 2010b; McDonnell *et al.* 2017). Moreover, IMS has become a valued technique in drug development to study

effects of pharmacotherapy, drug safety as well as for studying pharmacokinetics and drug metabolisms (Nilsson *et al.* 2015; Goodwin *et al.* 2016).

MALDI imaging MS is of particular relevance for protein and peptide analysis as it is to date the only IMS technique that has been demonstrated for robust *in situ* neuroproteomics and neuropeptidomics in single nerve cells (Kruse and Sweedler 2003; Rubakhin *et al.* 2003), invertebrate tissue (Hummon *et al.* 2006; Chen *et al.* 2010; Ye *et al.* 2013) as well as within rodent and human CNS tissue in a neurological disease context (Pierson *et al.* 2005; Monroe *et al.* 2008; Hanrieder *et al.* 2013b, 2015). It is, however, important to mention that there are of course very exciting developments, using other IMS modalities such as metal enhanced SIMS for neuropeptide imaging (Altelaar *et al.* 2006), the use of novel gas cluster ion sources for ToF-SIMS-based peptide detection as well as a DESI MS-based method for protein imaging (Feider *et al.* 2016) that all hold great promise for future applications.

Still, given the prominent role of MALDI IMS for imaging of neuropeptides and neuroproteins, the present review is focused on MALDI IMS. Herein, different concepts and challenges with respect to sample collection, tissue preparation, data acquisition and analysis as well as molecular validation are discussed. Finally, an overview of MALDI IMS applications for probing spatial protein and peptide regulations is provided with focus on applications to neurodegenerative disease pathology including Parkinson’s disease and in particular Alzheimer’s disease. There is a

number of recent reviews that focus on the more methodological parts of the technique as well as applications in other clinical disciplines (Dreisewerd 2014; Aichler and Walch 2015; Bodzon-Kulakowska and Suder 2016; Baker *et al.* 2017; Schwamborn *et al.* 2017; Vaysse *et al.* 2017). While the general aim of this review is to give a full picture of current developments, the authors apologize if not every study within the field is included.

MALDI imaging MS

During the 1990s, Bernhard Spengler and Richard Caprioli demonstrated the application of MALDI for spatial analysis of proteins and peptides in biological tissues (Spengler *et al.* 1994; Caprioli *et al.* 1997). In MALDI, as well as in ESI, molecular ions of large, intact biomolecules such as lipids, peptides and proteins can be transferred into the gas phase with minimal in source fragmentation as compared to other ionization techniques available before. In source fragmentation has, however, still to be considered as labile protein side groups such as various post translational modifications as well as sugar residues of glycolipids can dissociate during the laser desorption/ionization process. In conventional MALDI imaging, a UV light absorbing crystalline matrix is co-crystallized together with the sample, which facilitates desorption and ionization of intact large biomolecules upon irradiation with a UV laser beam (Karas and Hillenkamp 1988) (Fig. 1). Similarly, MALDI efforts using IR lasers and IR absorbing matrices have been presented that allow detection and imaging of intact proteins (Dreisewerd *et al.* 2007a,b).

MALDI is a quick, sensitive and robust technique that features a large molecular mass range and has been demonstrated for detection of large protein complexes up to 1MDa in weight (Wenzel *et al.* 2005). While this has not been entirely realized for *in situ* detection, MALDI imaging of large proteins up to ~70 kDa in weight has been demonstrated, although this required instrument modifications with a high mass detector (van Remoortere *et al.* 2010).

In contrast, the detection of smaller low-molecular weight molecules (< 500 Da) such as drugs, metabolites and neurotransmitters is challenging as the mass signals generated by the matrix interfere with those species. Several, elegant solutions to overcome this issue have been presented, including surface activated laser desorption/ionization (Northen *et al.* 2007) without any organic matrices as well as other strategies, including use of a stable isotope modified matrix or MS/MS methodologies and most elegantly by *in situ* derivatization as demonstrated for neurotransmitters in PD (Shariatgorji *et al.* 2014).

In MALDI IMS, a spatial resolution of 5–10 μm is typically achieved and was even demonstrated down to 1.4 μm , using a specially designed source setup (Kompauer

et al. 2017) or 1 μm using a transmission geometry source setup (Zavalin *et al.* 2015).

The spatial resolution of MALDI IMS is restricted by multiple parameters such as the focus of the laser, if not running in oversampling mode, as well as the size of the matrix crystals. In addition, lateral diffusion effects that can occur during the various sample preparation steps impact spatial resolution significantly (Spengler and Hubert 2002; Jurchen *et al.* 2005; Rompp *et al.* 2010; Kompauer *et al.* 2017). Furthermore, for each IMS experiment, practical consideration when choosing the spatial resolution need to be given to how many samples and what size of tissue areas are analyzed as high spatial resolution implies longer acquisition time and lower sample throughput.

In preparation to designing an imaging MS-based strategy for *in situ* detection of peptides and proteins, various parameters with respect to sample preparation have to be considered that will have significant impact on sensitivity, sample stability and data reproducibility, spatial resolution, molecular mass range of the target species and sample throughput.

Particular attention has been put on all parts of the sample preparation workflow for MALDI IMS that involves every step from tissue retrieval, tissue section collection, sample fixation and clean up followed by matrix application. All of these steps have therefore to be adjusted and optimized for each tissue type and most importantly, the molecular targets of interest.

Sample preparation for MALDI imaging of proteins and peptides

Sample collection

For all IMS experiments, tissue retrieval from animal- or human sources, as well as tissue storage, are most critical for data quality. Both chemically fixed tissue, such as formalin-fixed paraffin-embedded, and fresh-frozen tissue, can be analyzed with IMS, though fresh-frozen tissue is most commonly used. This is mainly due the fact that chemical perfusion and fixation strategies are not easily compatible with mass spectrometry-based analyses as these polymeric fixation and embedding agents, such as paraformaldehyde (PFA) and paraffin, do interfere with the MS detection. Still, elegant solutions to overcome these obstacles have been proposed, including *in situ* trypsinolysis following paraffin removal and antigen retrieval (Gustafsson *et al.* 2010; Meding *et al.* 2013). Furthermore, recent developments show successful detection of lipids and peptides (Pietrowska *et al.* 2016) and even metabolites (Buck *et al.* 2015; Urban *et al.* 2018) in formalin-fixed and paraffin-embedded specimen which is opening up tremendous opportunities for MALDI imaging-based histology studies on large pathological sample sizes that are available in tissue banks (Gorzolka and Walch 2014; Longuespee *et al.* 2014).

Yet, use of fresh-frozen tissue for molecular analysis of *ex vivo* tissue samples is still most common for IMS. Here, rapid freezing, leading to formation of amorphous, vitreous solid state of water, rather than the crystalline form, is crucial for preservation of protein integrity at cellular and subcellular, and general tissue morphology, which is otherwise compromised by cell wall rupture. Such instant ‘snap-freezing’ or ‘flash-freezing’, is typically carried out by submersion of freshly dissected tissue in liquid nitrogen. This maximizes the surface area of tissue that is in contact with the coolant and offers in principle the fastest rate of cooling. However, formation of a vapor barrier at the surface of warm tissue can result in uneven freezing. Therefore, liquid nitrogen cooled-, and sometimes dry ice cooled, isopentane is also used, in particular for larger specimens, such as whole rodent brains. Since postmortem delays of more than 3 min, result in severe degradation of neuropeptides (Goodwin *et al.* 2008), tissue isolation and freezing should be performed rapidly. Protein degradation, can be minimized using *ex vivo* heat stabilization strategies for protease inactivation (Goodwin *et al.* 2010). This, however, affects the morphology of the sample, making it less suitable for spatial molecular analysis. Cryosections from fresh-frozen tissues can then be collected on a cryostat microtome at -15 to -20°C and thaw-mounted within the cryostat onto metal targets or special glass slides with a conductive coating. Here, challenges arise from freeze damages caused by ice formation through condensation unless the tissues are dried directly before storage. (Hanrieder *et al.* 2012a).

Tissue section preparation

Following sample collection, tissue sections need to be prepared through appropriate sample clean up, such as washing, and application of the matrix. Here, the selection of appropriate washing protocols of the tissue sections is a critical step. Several washing steps using organic solvent/ aqueous solutions can be used in order to remove components that could interfere with the MS analysis and to enhance the signal quality of the analytes of interest. For lipid analysis, washing steps with organic solvents are omitted as these can result in delipidation. However, recently a cleanup protocol based on ammonium acetate was demonstrated for efficient desalting prior to lipid imaging resulting in enhanced signals for various lipid species (Wang *et al.* 2011). For imaging of drugs, neuropeptides and proteins advanced multistep washing protocols are typically employed prior to matrix application. These consist of pH optimized organic and aqueous washes, that aim to precipitate the peptides and proteins, remove lipids, and wash off salts that could interfere with the signal (Seeley *et al.* 2008; Hanrieder *et al.* 2012a; Shariatgorji *et al.* 2012). Several washing protocols have been evaluated for enhancing protein signals in MALDI imaging. Here, stepwise washing with gradient alcohol was found to give

the most significant improvement in signal quality (Seeley *et al.* 2008; Martin-Lorenzo *et al.* 2014).

Matrix application

For applying the matrix onto the tissue section, different approaches can be used such as nebulizer-based methods or micro-spotting with a chemical printer. Each method has its own strengths and limitations. While manual application with an airbrush nebulizer is the most straightforward and cost-effective solution, it is severely hampered by its lack in reproducibility as well its susceptibility to sample diffusion as well as limited extraction efficiency. However, commercially available nebulizer-based solutions (ImagePrep, Bruker Daltonics, Bremen, Germany; TM sprayer, HTX Technologies Carrboro, NC, USA; SunCollect, Sunchrome, Napa, CA, USA), as well as open access solutions (iMatrixSpray, (Stoeckli *et al.* 2014)), can help to overcome these challenges with respect to reproducibility as well as extraction efficiency. A further, even more controlled matrix application technique involves deposition of pL-droplets of the matrix solution, (micro-spotting). For this approach, a chemical inkjet printer can be employed (e.g., ChiP; Shimadzu, Kyoto, Japan) or alternatively, a pneumatic vertical spotter (Portrait; Labcite, Sunnyvale, CA, USA) can be used (Aerni *et al.* 2006; Baluya *et al.* 2007), although both setups are discontinued by their manufacturers. Due to the accurate and repetitive deposition of matrix droplets, challenges with lateral analyte diffusion as observed for nebulizer approaches are overcome (Aerni *et al.* 2006). In addition, these matrix micro-spotting technologies are superior in terms of sensitivity and reproducibility due to enhanced extraction, allowing *in situ* quantification of low abundant neuropeptides (Hanrieder *et al.* 2011). This is, however, at significantly lower spatial resolution due to the size of these micro-spots typically ranging in between 150 and 200 μm . Finally, an elegant methodology based on sublimation and recrystallization for protein imaging has been presented allowing straightforward and cost effective matrix application along with protein imaging at a high spatial resolution (Yang and Caprioli 2011).

A large variety of different matrices have been reported for MALDI IMS, where different matrices display preferential ionization properties for different kinds of analytes (for review see e.g., Norris and Caprioli 2013; Schwartz *et al.* 2003). Hence, the choice of matrix depends largely on the targeted substance. Matrix application method development aims to overcome distinct challenges of MALDI sample preparation with respect to crystal size, extraction efficiency, interfering matrix cluster, mass range as well as, most importantly, signal quality and reproducibility.

For protein and peptide analysis, the most prominently used matrices are 2,5-dihydroxy-benzoic acid (DHB) (Strupat *et al.* 1991; Schwartz *et al.* 2003), sinapinic acid (SA) (Beavis and Chait 1989), 2,5-dihydroxy acetophenone (2,5-

DHA) (Zavalin *et al.* 2015) and 4-hydroxy- α -cyano-cinnamic acid (HCCA) (Beavis *et al.* 1992). DHB-based MALDI IMS was demonstrated as a reliable approach for reproducible and sensitive neuropeptide imaging, using the micro-spotting approach (Hanrieder *et al.* 2012a). Further, HCCA and 2,5-DHA have been demonstrated as convenient approaches for MALDI IMS of peptides and small proteins. HCCA has limitations for larger protein species and displays extensive cluster formation, convoluting the lower mass range (< 700 Da), which in turn impacts detection of smaller compounds including small neuropeptides such as, e.g., Leu-enkephalin. 2,5-DHA and SA on the other hand allow detection of larger protein species; though 2,5-DHA is less stable in vacuum than SA, thereby limiting the overall acquisition time and throughput, respectively.

Finally, a common feature for all matrices that impacts spatial resolution and hence requires attentive optimization is the crystal size. This is mainly related to formation of too large droplets, i.e., too wet matrix application. In addition, some matrices like DHB form larger crystals than others. However, optimal solvent systems along with optimized parameters of currently used nebulizer setups allow to control for this issue. In addition, rather dry matrix application methods, including dry coating and sublimation result in a very small crystal size (Hankin *et al.* 2007; Puolitaival *et al.* 2008; Goodwin *et al.* 2011; Murphy *et al.* 2011; Thomas *et al.* 2012). While this allows for IMS at high spatial resolution, there are limitations as these methods typically show less efficient analyte extraction and limited suitability for protein imaging. Moreover, there are limitations with respect to analysis time and sample throughput as the matrices used are less stable in high vacuum. One solution to overcome the sensitivity issues includes sublimation along with matrix recrystallization, which was demonstrated to give significantly enhanced signal intensity for protein imaging (Yang and Caprioli 2011).

In summary, the different properties of the various matrices have to be taken into consideration, when designing the IMS experiments. Further, the solvents used in the matrix solution have to be optimized with respect to organic and hydrophilic solvent content along with acid and base additives to achieve the correct pH value allowing optimal extraction of the target species along with good solubility of the matrix compounds. Here, mixtures of water with acetonitrile, methanol, and ethanol are commonly used along with acetic acid, formic acid or tri-fluoro acetic acid and ammonium -bicarbonate, -acetate or -formate buffers for adjusting the pH value.

IMS data acquisition

Acquisition of IMS data involves the *in situ* desorption and ionization of molecular targets followed by ion separation and detection in a mass analyzer that allows to determine the mass to charge (m/z) ratio for the molecular targets of interest. As

MALDI is a discontinuous, pulsed ion source, ToF mass analyzers are most commonly used for ion separation and detection as these analyzers operate in a pulsed fashion as well and can therefore easily be implemented with the laser source. ToF analyzers, especially in conjunction with MALDI sources, provide high sensitivity, a large mass range and high acquisition speed at very good mass resolution and mass accuracy, respectively. The dominance of ToF analyzers for MALDI IMS is, however, changing as recent developments in source design and ion optics paved the way for other MALDI IMS architectures including hyphenation to FT (Fourier Transform) mass analyzers including orbitraps (Landgraf *et al.* 2009; Rompp *et al.* 2010) as well as Fourier transform ion cyclotron resonance iontraps (FTICR) (Taban *et al.* 2007; Spraggins *et al.* 2015; Dilillo *et al.* 2017; Prentice *et al.* 2018). These platforms feature tremendous improvements with respect to mass resolution and mass accuracy as well as MS/MS capabilities. This allows to retrieve amino acid sequence information of individual peptide and protein species *in situ* as well as for characterization of fatty acid patterns of lipids as recently presented with a very powerful approach for automated, in parallel MS/MS imaging (Ellis *et al.* 2018). Due to their high resolving power, FT mass analyzers are preferentially used within the pharmaceutical industry, where drugs are characterized by their intact mass and isotope pattern as reviewed in detail elsewhere (Prideaux and Stoeckli 2012). Beyond the development of FT analyzers other ToF-based architectures have become a recognized alternative. This includes MALDI qToF systems (Waters Synapt, Wilmslow, UK) that allow for ion mobility of desorbed ions prior to ToF-based detection. This can increase sensitivity and facilitate separation of isoforms and isobaric species, as well as provide structural information and enhance protein identification (Stauber *et al.* 2010). Other ToF-based systems include the spiralToF (Jeol, Peabody, MA, USA) that allows high mass resolution imaging (Muller *et al.* 2017) as well as the MALDI ion trap-ToF (Shimadzu Axima, Kyoto, Japan), which facilitates MS_n fragmentation and enhanced structural characterization, respectively (Shimma *et al.* 2008).

For state of the art MALDI imaging experiments, decisive factors involve sensitivity, selectivity and specificity at high spatial resolution and sample throughput. Commonly, these parameters do influence each other diametrically, such as that high spatial resolution results in limitations with respect to sensitivity and sample throughput. Consideration has therefore to be put on choosing a fair tradeoff in between these factors depending on the type of sample and study design for exploratory/pilot studies, mechanistic investigations or large-scale (pre)-clinical screenings.

Validation of IMS protein and peptide data

While IMS is a very powerful approach for comprehensive visualization of multiple proteins and peptides *in situ*,

complementary strategies for validation of the putatively identified peptides/proteins are needed. This includes validation and verification of both the putatively assigned peak identities that show potentially relevant spatial localizations as well as biological validation of the histopathological context. Mass peak identity validation is particularly relevant in IMS of intact proteins that are acquired in linear mode, where the mass accuracy and resolution of the ToF analyzer do not permit unambiguous identification based on the accurate mass. Further, one needs to take into consideration potential sources of bias inherent to the methodology, such as, for instance, suppression effects, which could result in false positive findings and wrong interpretation. For validating both, peak identity and potential histological context, mass spectrometry-based approaches are commonly used for *in situ* and off tissue characterization. Further, immunohistochemistry (IHC) as well as histological staining, are commonly employed as these provide both some orthogonal identity validation as well as spatial validation of the histological context for the peak localizations (Chaurand *et al.* 2004; Schwamborn and Caprioli 2010a).

Mass spectrometry-based identification

In IMS experiments of intact peptides and proteins, the individual species can be putatively annotated on the basis of the accurate m/z values and comparison to literature values. For protein and peptide identification, initial *in situ* validation of IMS data can commonly involve IHC analyses on the same or consecutive tissue sections as described in detail below. This approach can, however, be challenging, especially in cases of truncated protein isoforms, as the availability of the antibodies and their ability to differentiate between different isoforms can be limited. Given its molecular specificity, mass spectrometry-based tools are the methods of choice for protein identification and validation. The preliminary assignment of identified proteins is typically complemented with detailed analysis of the protein or peptide sequences. Here, a top-down fragmentation, directly on tissue, would in principle be the most convenient solution as this can verify protein/peptide identity and distribution directly *in situ*. However, *in situ* top down analysis is very challenging when it comes to identification of larger intact proteins, as post-source decay (PSD)-based MS/MS of proteins can lead to in-source fragmentation due to the increased laser energies used to generate metastable parent ions. Some efforts to overcome this issue have been presented by integrating an ESI source following laser desorption (laser ablation-electrospray ionization; LAESI) in order to generate multiply charged protein ions, which does provide a potential for further advancement of *in situ* fragmentation strategies (Kiss *et al.* 2014). A further, powerful strategy for *in situ* protein identification that can be implemented in the MALDI imaging experimental setup includes subsequent *in situ* digestion (Groseclose *et al.*

2007). Here, the MALDI IMS experiment of intact proteins is followed by application of an endoprotease solution (e.g., trypsin) onto the tissue sample, which is followed by imaging and fragmentation of the corresponding proteolytic peptides. The identified peptide species can then confirm the identity of the putatively assigned protein by showing the same spatial distribution pattern (Groseclose *et al.* 2007). This approach is a straightforward method to validate protein identities *in situ* but requires that the corresponding protein and its proteolytic degradation products have been well characterized before. Further, some concerns may arise with respect to lateral diffusion effects due to wet application and incubation with the enzyme solution, which may impact spatial resolution. This can, however, be mitigated by optimizing the instrumental settings. A further limitation when performing *in situ* MS/MS of proteolytic peptides is the number of fragmentation experiments (about $n=3$) that can be performed *in situ* within a distinct area. This limitation applies primarily with ToF/ToF setups, using post-source decay due to sample and matrix consumption as a consequence of higher laser energies that are needed for fragmentation. Another, commonly used approach for molecular identification is targeted isolation of histological features, using laser microdissection or diligent manual tissue dissection followed by multidimensional proteomics analysis of tissue extracts (Andersson *et al.* 2008; Hanrieder *et al.* 2012a; Carred *et al.* 2016).

Similarly, mass spectrometry-based analysis can be performed for endogenous peptide identification hence referred to as peptidomics. This approach is similar to proteomics but omits the endoprotease degradation step and involves typically a pre-fractionation strategy for peptide isolation such as mass cut-off filters (Skold *et al.* 2002; Svensson *et al.* 2003). For peptidomics, the most critical steps involve sample collection, peptide extraction, peptide fractionation and data analysis (Skold *et al.* 2002; Svensson *et al.* 2003; Hanrieder *et al.* 2012b). As mentioned above, fast tissue collection and snap-freezing are essential to avoid peptide degradation (Svensson *et al.* 2007; Goodwin *et al.* 2008). Here, the tissue homogenate solution is spiked with an internal standard, to account for technical variation introduced during the sample preparation (extraction, purification and pre-fractionation). Peptide separation and characterization is then performed with proteomic workflows, including one- or two-dimensional liquid chromatography coupled to ESI-MS/MS (Skold *et al.* 2002; Svensson *et al.* 2003). A particular challenge in peptidomics is the identification from MS/MS data as protein databases cannot be employed. This can be overcome by elaborate manual annotation of the MS/MS spectra and sequence homology analysis or by comparing to specifically designed peptide databases that contain numerous known neuropeptide sequences and *in silico*-generated or experimental peptide fragmentation data (Falth *et al.* 2006, 2007a,b).

Histological staining and immunohistochemistry

It is of great importance to put the comprehensive molecular information as provided by MALDI imaging in a pathohistological context. Here, histological assessments using either histological stains or epitope specific antibodies can be performed either on the adjacent section or on the on the same section that the MALDI imaging experiment was or will be performed on. Consecutive tissue staining is appropriate when looking at gross morphological features, such as for instance differences in brain white and gray matter, that are present across the tissue. No prior exposure to the MALDI imaging preparations enable use of both non-specific histological stains as well as epitope-directed antibodies (Walch *et al.* 2008). This approach is, however, not appropriate when looking at small features, such as protein inclusions or single cell layers, as these will simply be lost between sections. As a consequence, staining on the same tissue section is preferred.

Staining on the same tissue section can be executed either prior or after the MS analysis. Histological analysis prior to MALDI imaging offers great advantage for guided, spatially targeted IMS experiments that are less time consuming. For staining prior to IMS, one has to take into consideration a potential impact of the staining on the overall protein pattern (localization), protein signal intensity and the quality of the obtained spectrum (Chaurand *et al.* 2004). Therefore, appropriate controls need to be used when aiming to establish new histology-guided MALDI imaging protocols. Several simple histological stains, including alcohol-based Methylene Blue as well as water-based Cresyl Violet and Terry's Polychrome, have been demonstrated to be MALDI imaging compatible (Chaurand *et al.* 2004). On the other hand, commonly used hematoxylin and eosin (H&E) staining has been shown to severely impact mass spectra quality by interfering with protein signal (Nakanishi *et al.* 2005; Xu *et al.* 2016). Still, H&E staining is typically performed in the majority of MALDI imaging studies, but is done after mass spectra acquisition (Deutskens *et al.* 2011). While these histological staining approaches are suitable for gross evaluation of cell and tissue architecture, they are limited by their specificity.

In the context of neurodegenerative diseases, the use of conformation-specific antibodies, or antibodies directed towards large, non-easily ionized proteins, are often of interest. Antibody-based staining is, however, more elaborate than the histological stains mentioned above due to use of, for example protein-based blocking. IHC can therefore not be performed prior to MALDI imaging. On the other hand, IHC following IMS acquisition can also be hampered due to laser-induced tissue distortion, and associated epitope degradation (Vogel and Venugopalan 2003; Russo *et al.* 2013; Kaya *et al.* 2017c).

Recently, some interesting approaches have been developed for correlative optical/microscopy and MALDI-based

imaging. Here, Lavenant *et al.* (2013) described an integrative IMS/IHC approach, using a targeted, multiplex IMS assay based on photo-cleavable mass-tags bound to primary antibodies. Still, while the method in principle enables indirect visualization of any predefined target, it is limited by its interference of non-targeted endogenous proteins. Further, Kaya *et al.* (2017c) demonstrated a comprehensive imaging paradigm that employs a MALDI matrix that requires only low laser fluences for ionization and in turn facilitates histology compatible MALDI IMS of lipids as well as for subsequent fluorescent, immunohistological imaging on the same tissue sample. While this approach is well suited for IMS of lipids, comprehensive analysis of peptides and proteins is more challenging as desorption and ionization of protein and peptides require higher laser fluences leading to tissue distortion effects (Kaya *et al.* 2017c). Therefore, a suitable matrix is required that is easy to ionize and requires lower laser energies. Moreover, the introduction of washing protocols prior to protein and peptide analysis, as described above, need optimization as these influences downstream IHC staining significantly.

For lipid imaging data, biological validation with subsequent IHC can be complemented with consecutive protein and peptide imaging MS on the same section. Here, repeated matrix deposition and trimodal IMS analysis (IMS3) has been demonstrated to reveal amyloid beta (A β) plaque pathology-associated anionic- and cationic lipid accumulations along with the distinct A β peptide patterns in a transgenic AD mouse model. This approach overcomes the need for antibody-based confirmation of A β peptide species that co-localize with the IMS identified lipid species and indeed provides even superior specificity and comprehensiveness compared to IHC staining experiments (Kaya *et al.* 2017a, 2018).

Data analysis

Given the immense complexity of IMS data sets, a cornerstone of the IMS workflow is the application of appropriate tools for data analysis. Here, multiple multivariate analysis (MVA) tools, can be employed to probe IMS data sets for unbiased segmentation (Deininger *et al.* 2008; Henderson *et al.* 2009; Graham and Castner 2012; Hanrieder *et al.* 2013a). In essence, this approach treats every pixel spectrum as individual sample in multivariate space and uses multivariate statistics to identify the most prominent variation and co-variation, respectively, that is then captured in the respective factor of the analysis. From the corresponding loading values, the variables, i.e., mass peaks and their intensity that contribute most to the variation captured in the factor are retrieved.

Similarly, cluster analysis tries to identify similarities that allow to group pixel spectra based on similar traits that essentially relate to similar peak patterns. With this approach, chemical differences and similarities can be identified across

the imaged tissue region. The aim is then to correlate chemical patterns retrieved by the statistics to anatomical features and ROI for subsequent, targeted, comparative statistical analysis of ROI spectral data. Multivariate data analysis methods have shown to be powerful tools for unsupervised data mining for exploratory purposes, and for supervised classification as applied in biomarker discovery (Bonnell *et al.* 2011; Alexandrov 2012). Principal component analysis (PCA) (Fonville *et al.* 2012), hierarchical cluster analysis (Maccarrone *et al.* 2017) and non-negative matrix factorization (NMF) (Jones *et al.* 2012) have been applied. However, many studies report combinations of MVA methods such as PCA and hierarchical cluster analysis (De Sio *et al.* 2015) PCA and maximum autocorrelation factor analysis (MAF) (Hanrieder *et al.* 2013a) or PCA, NMF, MAF, and probabilistic latent semantic analysis (PLSA) (Race *et al.* 2016). Race *et al.* (2016) highlight in their communication how a combination of multivariate statistical tools in a complementary fashion aid interpretation of MALDI MS images of sagittal sections of rat brain. Moreover, correlation analysis has been applied on MALDI image data (Fülöp *et al.* 2016), in order to correlate information between MALDI and complementary imaging experiments such as Raman imaging (Bocklitz *et al.* 2013; Masyuko *et al.* 2013).

The analysis of IMS data usually requires preprocessing of the raw spectral data in order to reduce experimental variance within the data set and, thereby, prepare them for subsequent statistical analysis. Except for additional spatial coordinates, spectral image data do not differ much from single measurement data and thus, similar preprocessing procedures can be applied. The most important spectra processing steps include baseline correction, intensity normalization, smoothing, recalibration and alignment of spectra (Norris *et al.* 2007). Here, recalibration and alignment is of particular importance when subjecting the data to MVA methods for data analysis. For processing, visualization and evaluation of IMS data, a number of commercial software and freeware packages have

been developed. Table 1 summarizes commercially available IMS software packages and their distinct features for data analysis. Many of the available freeware/open access IMS software packages are toolboxes for MATLAB (Mathworks Inc., Natick, MA, USA) or packages for R (R Foundation for Statistical Computing, Vienna, Austria) and are listed in detail in Table 2. All of these software packages and toolboxes enable qualitative IMS analysis through visualization functions. Spectral data preprocessing algorithms are included to various degrees and some have been developed for quantitative IMS analysis (*MALDIquant*, *msIQuant*, *Quantinetix*). A number of packages exhibit capacities for multivariate analysis of image data, in various extent (e.g., *Cardinal*, *massPix*, *MIA_Toolbox*, *SCiLS Lab*, *SpectralAnalysis*). Qualitative comparative analyses of IMS data commonly include overlaying or blending together single ion images. Often, imaging data obtained with other techniques are registered and overlaid with MS images. Integrative interpretation across the modalities is, however, largely left to human judgment. An elegant solution of this included image fusion that combines the information from two modalities through predictive integration to generate images with superior information (Van de Plas *et al.* 2015). The fusion process applies partial least square (PLS) regression modeling linking variations between the modalities to then produce cross-modality estimations (Juan 2018; Prentice *et al.* 2018). In this way, MALDI IMS and optical imaging data can be fused to obtain predictions of ion distributions in tissues at the (higher) microscopy resolution and image sharpening, respectively. Van de Plas *et al.* (2015) demonstrated MALDI IMS/microscopy fusion on various tissue sections. Beside IMS data, fusion can be performed on data from various imaging techniques, such as FT infrared spectroscopy (FTIR), Raman, fluorescence, among others, and is an excellent way to exploit their complementary information, circumvent their limitations, and furthermore open doors to new biological understanding (Tarolli *et al.* 2014; Piqueras Solsona *et al.* 2017).

Table 1 Commercial MALDI IMS software packages

Software	Features	Vendor	Release year
flexImaging	2D visualization of ion distribution	Burker Daltonics	2005
HD Imaging	Visualization of IMS data, comparative analysis, multimodal IMS, image registration of multimodal IMS data	Waters Corp.	2011
ImageQuest	Visualization of imaging data in 2D and 3D	Thermo Fisher Scientific	2007
MALDIVision	IMS data visualization in 2D and 3D, comparative analysis, image registration (optical image to IMS data)	Premier Biosoft	2012
MIA_Toolbox	Comprehensive multivariate statistical analysis of IMS data	Eigenvector Research, Inc.	2005
Quantinetix	IMS data visualization and quantitative analysis	Imbiotech	2012
SCiLS Lab	IMS data visualization in 2D and 3D, comparative analysis, correlation analysis, classification modeling, spatial segmentation with annotation	Bruker Daltonics	2013

Table 2 Freeware/open access software packages for MALDI IMS

Software	Features	Release year	References
Biomap	Processing and visualization of IMS data and further imaging modalities	1996	Rausch and Stoeckli (2000)
Cardinal	R package, IMS data visualization, spectral data preprocessing, PCA, PLS-DA, classification, spatial segmentation	2015	Bemis <i>et al.</i> (2015)
DataCube Explorer	Visualization and qualitative analysis of IMS data	2013	Klinkert <i>et al.</i> (2014)
MALDIQuant	R package, IMS data visualization, spectral data preprocessing, quantitative analysis	2012	Gibb and Strimmer (2012)
<i>massPix</i>	R package, IMS data visualization, putative lipid annotation, classification, PCA, <i>k</i> -means clustering	2017	Bond <i>et al.</i> (2017)
Mirion	Visualization and automatic processing of MS image data	2013	Paschke <i>et al.</i> (2013)
mslQuant	Qualitative and quantitative analysis of IMS data, spectral preprocessing, calibration, analysis of very large data sets (> 50GB)	2016	Källback <i>et al.</i> (2016)
MSiReader	MATLAB tool, reading of various IMS data file formats, visualization of IMS data, spectral preprocessing	2013	Robichaud <i>et al.</i> (2013)
Omnispect	MATLAB tool for visualization and qualitative analysis of IMS data	2013	Parry <i>et al.</i> (2013)
OpenMSI	Web-based tool for the visualization, qualitative analysis and management of IMS data	2013	Rübel <i>et al.</i> (2013)
rMSI	R package for IMS data visualization and qualitative analysis	2017	Ràfols <i>et al.</i> (2017)
SpectralAnalysis	MATLAB tool, visualization and qualitative analysis of IMS data, spectral preprocessing, PCA, NMF, MAF, PLSA	2016	Race <i>et al.</i> (2016)
SpectViewer	IMS data visualization, assistance to data interpretation, classification, image registration and overlay	2014	Marie-France <i>et al.</i> (2014)

IMS, imaging mass spectrometry; MALDI, matrix-assisted laser desorption/ionization; MS, mass spectrometry; NMF, non-negative matrix factorization; PCA, principal component analysis; PLSA, probabilistic latent semantic analysis.

MALDI IMS applications to investigate CNS disease pathology

Imaging MS offers the possibility to in detail investigate components of various biomolecular pathways underlying many neurodegenerative diseases. This is particularly relevant for MALDI IMS, which allows to probe spatial concentration changes of peptides and small proteins. Indeed, misfolding and aggregation into potential neurotoxic deposits is a seminal histopathological occurrence for many major neurodegenerative diseases. This includes formation of alpha synuclein (aSyn) containing inclusions, Lewy bodies, in Parkinson's disease; Huntingtin in Huntington's disease; TDP43 in ALS and most prominently beta-amyloid plaques and hyperphosphorylated Tau tangles in Alzheimer's disease (Taylor *et al.* 2002). Moreover, several neurodegenerative as well as psychiatric disorders are accompanied by interference in neuropeptide mediated signaling circuits. Hence, MALDI IMS is a very well-suited approach to interrogate neuropeptide and protein dynamics *in situ* to further our mechanistic understanding of these diseases.

Parkinson's disease

Indeed, previously, MALDI IMS was successfully employed to delineate neuropeptide mediated motor control signaling circuits in PD and L-DOPA pharmacotherapy-induced

dyskinesia (Hanrieder *et al.* 2011, 2012a; Ljungdahl *et al.* 2011) These motor circuits are mediated by opioid peptides (dynorphins and enkephalins) and a striatal increase of prodynorphin (PDyn) mRNA has previously been associated with LID. The distinct PDyn processing products could not be characterized, using conventional techniques such as IHC due to lack of specific antibodies, which is a common challenge in *in situ* neuropeptide analysis. This specificity issue is particularly relevant to opioid peptides that differ in only a few C-terminal amino acids, which compromises the reliability of immunohistochemistry results significantly. In contrast, neuropeptide detection with mass spectrometry provides significant advantages with respect to molecular specificity, comprehensive detection (multiplexing) as well as throughput. A major consideration for IMS is the use of appropriate control experiments to account for the inherent inter and intra sample biological variation as well as technical reproducibility introduced due to sample preparation artefacts and ion suppression issues. One possibility to account for these variations is to use hemispheric disease models such as the unilateral nigrostriatal lesion with 6-hydroxy-dopamine model of PD (Ungerstedt 1968). As PD pathology in these animals develops only in one hemisphere the other hemisphere can serve as an optimal internal control for normalization. With this approach, spatial changes in secretion of PDyn derived opioid peptides were investigated in

LID in experimental PD (Hanrieder *et al.* 2011; Ljungdahl *et al.* 2011).

This revealed a significant increase for two dynorphin peptides, including dynorphin B and alpha neoendorphin, in the dorsal lateral striatum in high dyskinetic animals but not for low dyskinetic animals along with a strong positive correlation of both dynorphin species with LID severity. Further, this study revealed a selective metabolization of dynorphin peptides to des-tyrosinated species in the striatum of LID rats that could not have been delineated *in situ* using other imaging technologies, which further highlights the significant superiority of IMS with respect to its molecular specificity. Furthermore, this study described a brain structure specific *in vivo* metabolization of these dynorphin peptides where the N-terminal tyrosine was removed which was in addition associated with LID (Hanrieder *et al.* 2011; Ljungdahl *et al.* 2011). Interestingly, these des-tyrosine opioids can bind to other receptors pointing to other LID-associated signaling mechanisms (Walker *et al.* 1982). This further highlights the potential of MALDI IMS for neuropeptide imaging, as this *in vivo* metabolization cannot be detected with antibody-based techniques.

Further, MALDI IMS was demonstrated for to probing protein regulations in 6-hydroxy-dopamine PD mice, where ubiquitin (Ubc), and neurofilament M an axonal protein were found to be downregulated in PD rat brain, indicating axonal dysfunction as well as impaired protein turnover (Stauber *et al.* 2008). MALDI IMS has further been successfully applied for protein imaging in another neurotoxin-induced animal model of PD where IMS was employed to study striatal protein localization in 1-methyl-4-phenyl-1,2,3,6-tetrahydropyridine injected rats. Here, MALDI imaging revealed a striatal decrease of the neuronal calmodulin binding protein Pep19, which suggests that altered calcium homeostasis might be associated with neuronal cell death in this model (Skold *et al.* 2006). More recently, the Andr n lab reported groundbreaking data, where MALDI IMS was used to delineate brain wide neurotransmitter and amino acid regulations in experimental PD models in rats and monkeys (Shariatgorji *et al.* 2014). While not strictly protein centric, the data provide significant insight into brain structure-specific neurotransmitter concentration changes and metabolization in neurodegenerative disease pathology as well as in response to pharmacotherapeutic interventions.

Alzheimer's disease

Given the distinct use of MALDI IMS for comprehensive, *in situ* peptide imaging, the technology is a particular powerful tool to probe beta-amyloid (A β) peptide dynamics in Alzheimer's disease. Using this approach, A β truncations in individual plaques have been characterized in amyloid precursor protein (APP23) transgenic mice (Stoeckli *et al.* 2002; Seeley and Caprioli 2008). The authors reported a significantly higher content of A β 1–40 than A β 1–42.

Similarly, our group reported a comprehensive study on profiling brain-wide A β profiles in transgenic animals carrying the Swedish and Arctic mutation of APP (tgArcSwe) (Fig. 2a–f) (Carlred *et al.* 2016). In this study, we employed a multivariate image analysis approach to outline pathological features that constitute A β plaque pathology and reveal the associated A β profiles in individual deposits with different areas of the brain. Moreover, other plaque-associated proteins were identified within the same experiment, including microglial derived macrophage inhibitory factor (Carlred *et al.* 2016).

In another study on a triple-transgenic animal model of AD (3xtg), MALDI IMS revealed an AD pathology-associated decrease of neurogranin (Esteve *et al.* 2017). This is of particular interest, as the synaptic protein neurogranin, has been demonstrated to be a potential biomarker reflecting AD pathology-associated neurodegeneration in CSF (Kvartsberg *et al.* 2015). Finally, working on 5xFAD mice, Schwartz *et al.* (2015) reported intriguing results on enhancing low abundant A β signals such as A β 1–22 and A β 1–26 using optimized parameters for random projections PCA-based multivariate image analysis.

The potential for probing A β pathology in human AD tissue was recently demonstrated by two groups, where amyloid peptide profiles of individual plaques were delineated (Kelley *et al.* 2016a,b; Kakuda *et al.* 2017) (Fig. 2). In a recent study, Kakuda *et al.* demonstrated that A β 1–42 and A β 1–43 were selectively accumulated in senile plaques. In contrast, C-terminal truncated A β species (A β 1– x ; with $x = 36–41$) preferentially localized to leptomeningeal blood vessels (pia mater and arachnoid). Moreover, they delineated depositions of N-terminally truncated A β 40/42, including pyroglutamate of Glu-3 (A β 3pE-4x), where A β 40 peptides (A β 1–40 and A β 3pE-40) deposited to leptomeningeal vessels and A β 1–42 and A β 3pE-42 characteristically localized to senile plaques in the cerebral parenchyma (Fig. 3g–n). In addition, it was demonstrated that one C-terminal changes of a single amino acid between A β 1–42 and A β 1–41 results in significant distribution changes presumably due to the difference in the self-aggregation propensity of different C-terminal A β species. These differences in aggregation propensity are attributable to alterations in the peptides' hydrophobicity. In the light of this, neuronal lipids have been implicated in mediating A β aggregation dynamics via hydrophobic interactions, particularly as APP is a membrane protein with large hydrophobic transmembrane domains that encapsulates the A β sequence. Moreover, the E4 allele of the gene encoding the lipid transporter protein apolipoprotein E represents the most significant genetic risk factor to develop sporadic AD. Elucidating its potential role of plaque pathology-associated lipid species has, therefore, gained great attention in AD research. Indeed, our group has demonstrated multiple efforts to delineate plaque pathology-associated lipid species using MALDI Imaging (Kaya *et al.*

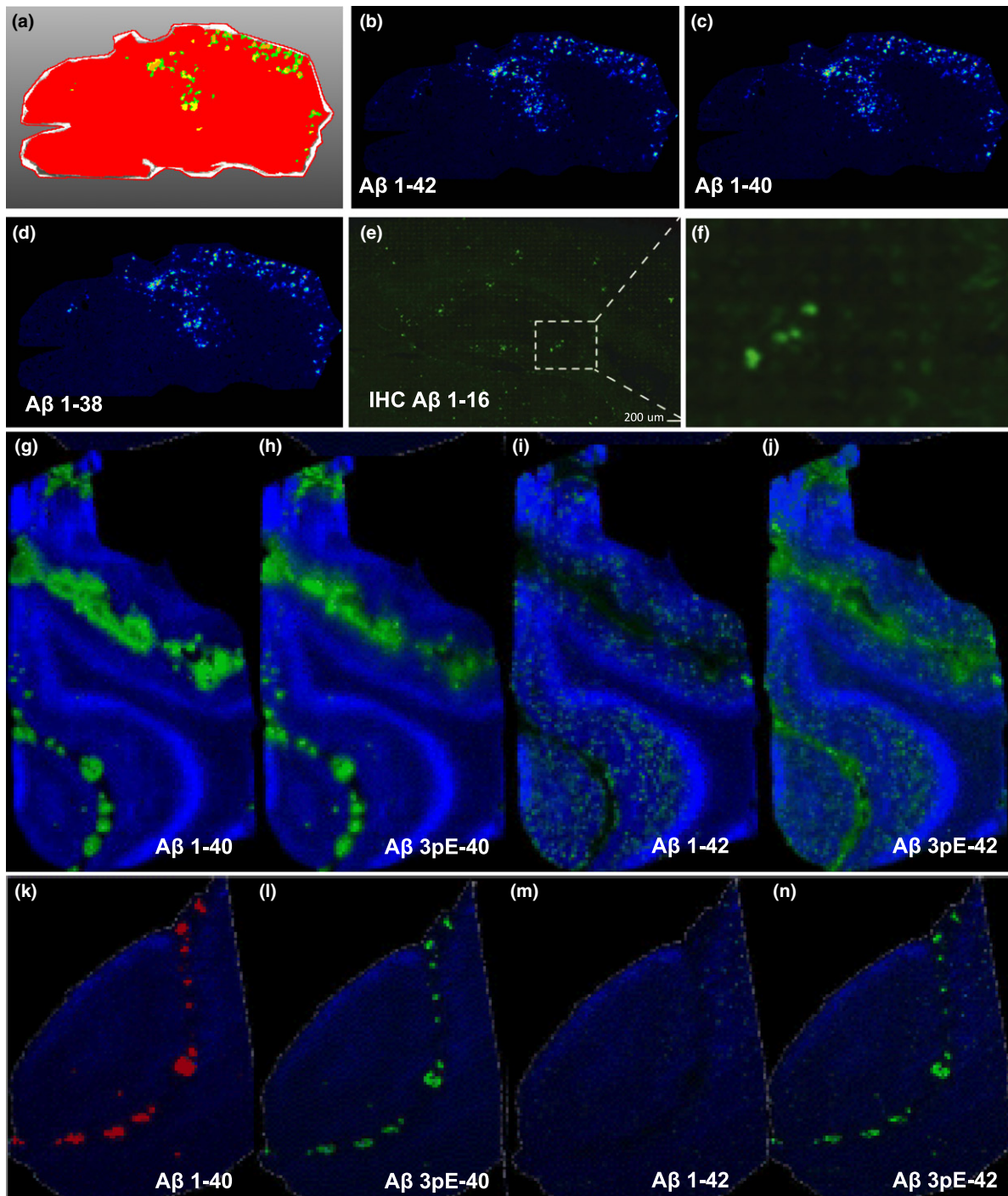


Fig. 2 MALDI Imaging of Amyloid Peptides in transgenic Alzheimer's disease (AD) mice. IMS experiments were performed for characterizing the plaque pathology in 18-month old transgenic AD mice (tgAP-PArcSwe). (a) Image analysis using hierarchical cluster analysis (bisecting k-means) delineates histological features resembling plaque pathology (yellow, green). (b–d) Inspection of the corresponding variables in the clusters that cause this difference, reveals major A β species. (d) The IMS staining experiments were complemented with

immunohistochemistry toward A β on the same section to verify the A β identity of these plaques in general (e: scale 1 mm; f: 200 μ m). (g–n) MALDI imaging of A β pathology human AD. Spatial patterns of A β 1–40/42 and N-term. A β 3–4 \times pyro-glutamate (3pE-A β 40/42) were detected at a 100 μ m (g–j) and 20 μ m resolution (k–n). A β 1–40 and 3pE-A β 40 showed preferential deposition to leptomeningeal blood vessels and arterioles (g, h, k, and l). In contrast, A β 1–42 and N3pE-A β 42 localized primarily to senile plaques in the cerebral parenchyma (i, j, m and n).

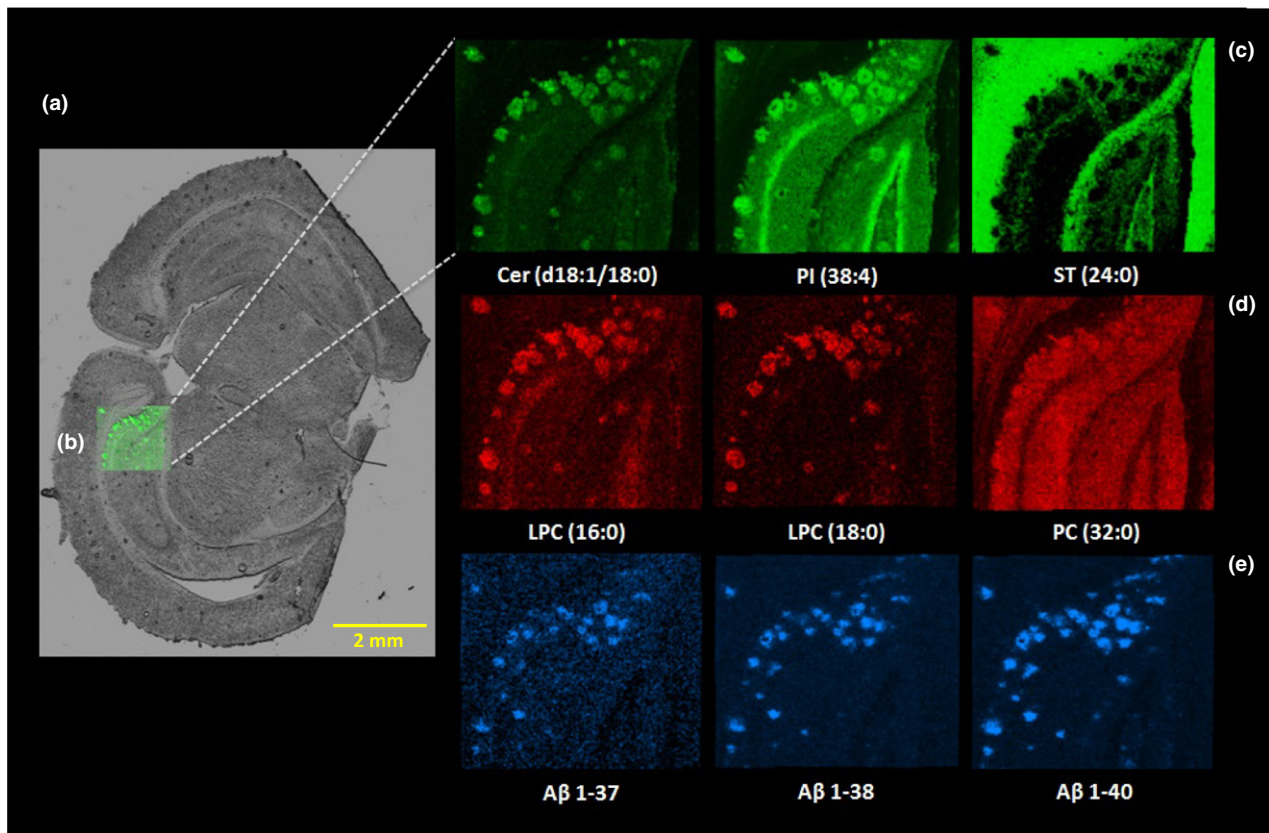


Fig. 3 Trimodal MALDI imaging of A β plaque pathology. Hippocampal amyloid plaque-associated lipids in dual polarity and peptides (a) on a coronal mice brain tissue section of transgenic Alzheimer's disease mice (tgArcSwe) were revealed by multimodal MALDI IMS. (b) The hippocampal region analyzed with 10 μ m spatial resolution. (c) Ion images of lipids: ceramides (Cer d18:1/18:0, m/z 564.6),

phosphatidylinositols (38:4, m/z 885.6), sulfatides (ST 24:0, m/z 890.6) in negative polarity (green) and (d) lysophosphatidylcholines (LPC 16:0, m/z 496.3, LPC 18:0, m/z 524.3) and phosphatidylcholines (PC 32:0, m/z 734.6) in positive (red) polarity with (e) subsequent amyloid- β (A β 1–37, m/z 4002.7, A β 1–38, m/z 4060.3, A β 1–40, m/z 4257.6) peptide (blue) ion images in the same imaging region.

2017a,b,c). Moreover, in order to elucidate the interaction of lipid and A β structures *in situ*, we expanded the MALDI IMS toolbox toward multimodal, three-step, imaging MS of both lipids and proteins on the same imaging array on the same tissue section based on the histology compatible setup introduced for multiplexed IMS and IHC experiments (Kaya *et al.* 2017a,c). The resulting trimodal MALDI IMS dataset revealed lipid and A β peptide correlates such as several sphingolipids, phosphoinositols and lysophosphatidic acids that have all been previously mechanistically implicated in AD pathology (Kaya *et al.* 2017a) (Fig. 3). Along the same track, a recent work established the association of lipids in A β polymorphism. Here, lipid imaging of diffuse cored A β plaques identified, that these morphologically heterogeneous A β deposits, displayed different lipid patterns. This in turn was tied to changes in A β 1–40 levels (Michno *et al.* 2018).

Other neurodegenerative and psychiatric disorders

Beyond the most prevalent neurodegenerative diseases (AD and PD), imaging MS was successfully demonstrated for

probing *in situ* protein changes in other neurodegenerative disorders including Huntington's disease; ALS and multiples sclerosis as well as psychiatric diseases. Here, MALDI IMS identified thymosin beta 4 to be specifically located to chronic active, demyelinated or only partly remyelinated multiples sclerosis lesions in white matter, suggesting a prominent role of thymosin beta 4 in migration and recruitment of immune cells underlying the autoimmune mechanisms leading to demyelination (Maccarrone *et al.* 2017). Further, MALDI imaging was used to probe huntingtin (Htt) aggregation dynamics in a mouse model of Huntington's disease upon treatment with a 23aa sequence of Htt (p42), previously shown to inhibit Htt aggregation (Arribat *et al.* 2014).

In context of ALS, MALDI Imaging enabled probing protein distributions in post mortem spinal cord tissue from ALS patients. (Hanrieder *et al.* 2012a) Here, an ALS-associated decrease of C-terminally truncated ubiquitin (Ubc 1-74; Ubc -G75G76) in the ventral horn, which could indicate changes in local protein turnover associated with

ALS pathology, was identified. Again, this highlights the potential of MALDI IMS over other immunohistochemical techniques to distinguish between various peptide isoforms. Other studies reported the use of MALDI IMS to probe brain wide protein changes in response to exposure with environmental neurotoxins that have been associated with neurodegenerative disease pathology. Here, Karlsson *et al.* studied hippocampal- and striatal changes in adult rats following neonatal exposure to the cyanobacterial toxin beta-methylamino-L-alanine (BMAA) (Karlsson *et al.* 2012, 2014). This toxin has previously been associated with the over represented development of ALS and PD like pathology in exposed populations and neonatal BMAA was found to induce neurodegeneration and formation of protein lesions in the CA1 region in the adult hippocampus of rats that were exposed to a high dose of BMAA neonatally (Karlsson *et al.* 2012). Using MALDI IMS in this model, the authors identified a BMAA-associated decrease in striatal myelin basic protein levels, presumably indicating denervation (Karlsson *et al.* 2014). Moreover, a selective increase of S100beta and histones was observed in the CA1 of BMAA animals indicating astrogliosis, while neurogranin was decreased in the CA1 and DG most likely reflecting axonal degeneration (Karlsson *et al.* 2012).

In addition to probe neurodegenerative disease pathology, the potential of MALDI IMS for neuropeptide and protein imaging is of value for studying molecular changes associated with psychiatric diseases. For instance, MALDI IMS was employed to characterize neuropeptide signaling circuits in addiction (Hishimoto *et al.* 2016). Here, substance P and proenkephalin projections were investigated upon nicotine administration, which revealed correlating changes in processing of the associated neuropeptide species. Similarly, MALDI IMS was successfully employed to probe neuropeptide changes in cocaine-sensitized rats (Uys *et al.* 2010). Here, the secretogranin II derived neuroactive peptide secretoneurin was identified to be increased in the nucleus accumbens upon cocaine administration. This is of interest as secretoneurin-modulated dopamine release and has been implicated in cocaine-induced mechanism of reward seeking (Schmidt *et al.* 2006).

Final discussion and perspectives

The majority of neurodegenerative diseases are associated with changes in protein dynamics, resulting in progressive accumulation of misfolded proteins into intra and/or extra cellular aggregates (Taylor *et al.* 2002). To delineate the molecular mechanism underlying these pathochemical alterations is often limited by the lack of biochemical tools that simultaneously offer the sensitivity and specificity, while maintaining the necessary spatial- and temporal resolution. This is particularly of interests when potential targets are unknown, or when differential production and enzymatic

processing of proteins and peptides might underlie the aggregation properties of these species, and their role in different stages of the pathology and disease.

Here, IMS and MALDI IMS in particular have on multiple occasions been demonstrated to delineate spatial information of protein and peptide distributions in pathological brain. As discussed in detail in the previous section, MALDI IMS has revealed selective production and processing of neuropeptides and proteins associated with different neurodegenerative mechanisms. For instance, MALDI IMS has provided novel insight in accumulation patterns of different A β peptide truncations in plaques from different brain regions, linking the differential A β peptide pattern to brain-wide disease progression. Further, while not strictly A β peptide centric, multimodal lipid- and protein IMS identified spatial lipid correlates associated with A β plaque pathology in AD.

MS imaging has made major advances within the last years with respect to performance, robustness and accessibility. As a result, the technique is becoming more and more applicable for biomedical and clinical research. Continuous improvements within instrumental design, robust sample preparation and advanced data analysis, facilitating implementation and comprehensive interrogation of multimodal imaging datasets, have been major factor driving this implementation. Moreover, a newly formed consortium of key leaders within imaging MS has released publishing guidelines for reporting IMS data, which makes the research findings from IMS more reliable and standardized. (McDonnell *et al.* 2015). Despite these developments, the final breakthrough of IMS in biological- and clinical research as well as in clinical routine is still imminent. This relates to two major challenges for introducing IMS to research and clinical settings. These challenges comprise a) full control of the whole IMS setup and sample preparation workflow from sample collection to data analysis and b) appropriate design of IMS-based studies with specialized hypotheses to test. The consequences arising from the first issue are to a greater extent outlined in the different chapters above. In sum, challenges concerning biological and technical variations are inherent to IMS-based experiments due to sample preparation and ion suppression effects. Hence, only full control of all aspect of the entire IMS workflow along with appropriate control experiments facilitates collection of high quality- and reproducible - data that allow for correct biological interpretation. This elutes directly into the second challenge, to address biologically relevant hypotheses beyond the assumption that 'there is a change' in molecular composition likely associated with the disease pathology under investigation. Given the inherent technical challenges of IMS and suppression effects in particular, such changes can be artefacts of sample preparation as well as due to concomitant histological factors such as a strong hemoglobin signal associated with vascular structures resulting in suppression of other localized proteins. While this calls for appropriate controls as to account for

these artifacts, it further highlights the need to tailor the IMS approach after the biological hypothesis in question. The different IMS modalities, with their complementary application profile, can be employed to target distinct chemical species and to elucidate their role in corresponding biomechanisms, as discussed above. When used appropriately, along with a well-defined and controlled study design, IMS can serve as a powerful technology to probe biological mechanisms and to further our mechanistic understanding of neurodegenerative disease pathology. Moreover, identification and validation of mechanistically implied novel molecular species can inform the development of pathology-associated biofluid- and imaging-based biomarkers for neurodegenerative diseases that have great relevance for monitoring neurodegenerative pathology, both, in clinical routine as well as for the development of pharmacotherapy approaches.

In summary, IMS is a powerful tool that can provide essential novel insight complementary to established microscopic techniques and highlight the protein and peptide dynamics crucial in progressing neuropathology.

Acknowledgments and conflict of interest disclosure

Funding was provided by The Swedish Research Council VR (no. 2014-6447, JH; no. 2013-2546, HZ; no. 2017-00915, KB), Alzheimerfonden (JH, KB), Demensfonden (JH), Hjärnfonden (KB), Jeansson's Stiftelsen (JH), Åke Wiberg Stiftelse (JH), Ahlén Stiftelsen (JH), Stiftelsen Gamla Tjänarinnor (JH, KB, WM), Torsten Söderberg Foundation (KB). The authors declare no conflict of interest.

References

- Aebersold R. and Mann M. (2003) Mass spectrometry-based proteomics. *Nature* **422**, 198–207.
- Aerni H. R., Cornett D. S. and Caprioli R. M. (2006) Automated acoustic matrix deposition for MALDI sample preparation. *Anal. Chem.* **78**, 827–834.
- Aichler M. and Walch A. (2015) MALDI imaging mass spectrometry: current frontiers and perspectives in pathology research and practice. *Lab. Invest.* **95**, 422–431.
- Alexandrov T. (2012) MALDI imaging mass spectrometry: statistical data analysis and current computational challenges. *BMC Bioinformatics* **13**, S11.
- Altelaar A. F., Klinkert I., Jalink K., de Lange R. P., Adan R. A., Heeren R. M. and Piersma S. R. (2006) Gold-enhanced biomolecular surface imaging of cells and tissue by SIMS and MALDI mass spectrometry. *Anal. Chem.* **78**, 734–742.
- Andersson M., Groseclose M. R., Deutch A. Y. and Caprioli R. M. (2008) Imaging mass spectrometry of proteins and peptides: 3D volume reconstruction. *Nat. Methods* **5**, 101–108.
- Arribat Y., Talmat-Amar Y., Paucard A. *et al.* (2014) Systemic delivery of P42 peptide: a new weapon to fight Huntington inverted question marks disease. *Acta Neuropathol. Commun.* **2**, 86.
- Aslund A., Sigurdson C. J., Klingstedt T. *et al.* (2009) Novel pentameric thiophene derivatives for in vitro and in vivo optical imaging of a plethora of protein aggregates in cerebral amyloidoses. *ACS Chem. Biol.* **4**, 673–684.
- Baker T. C., Han J. and Borchers C. H. (2017) Recent advancements in matrix-assisted laser desorption/ionization mass spectrometry imaging. *Curr. Opin. Biotechnol.* **43**, 62–69.
- Baluya D. L., Garrett T. J. and Yost R. A. (2007) Automated MALDI matrix deposition method with inkjet printing for imaging mass spectrometry. *Anal. Chem.* **79**, 6862–6867.
- Beavis R. C. and Chait B. T. (1989) Cinnamic acid derivatives as matrices for ultraviolet laser desorption mass spectrometry of proteins. *Rapid Commun. Mass Spectrom.* **3**, 432–435.
- Beavis R. C., Chaudhary T. and Chait B. T. (1992) α -Cyano-4-hydroxycinnamic acid as a matrix for matrix-assisted laser desorption mass spectrometry. *Org. Mass Spectrom.* **27**, 156–158.
- Bemis K. D., Harry A., Eberlin L. S., Ferreira C., van de Ven S. M., Mallick P., Stolowitz M. and Vitek O. (2015) Cardinal: an R package for statistical analysis of mass spectrometry-based imaging experiments. *Bioinformatics* **31**, 2418–2420.
- Bocklitz T. W., Crecelius A. C., Matthäus C., Tarcea N., von Eggeling F., Schmitt M., Schubert U. S. and Popp J. (2013) Deeper understanding of biological tissue: quantitative correlation of MALDI-TOF and Raman imaging. *Anal. Chem.* **85**, 10829–10834.
- Bodzon-Kulakowska A. and Suder P. (2016) Imaging mass spectrometry: instrumentation, applications, and combination with other visualization techniques. *Mass Spectrom. Rev.* **35**, 147–169.
- Bond N. J., Koulman A., Griffin J. L. and Hall Z. (2017) massPix: an R package for annotation and interpretation of mass spectrometry imaging data for lipidomics. *Metabolomics* **13**, 128.
- Bonnel D., Longuespee R., Franck J., Roudbaraki M., Gosset P., Day R., Salzet M. and Fournier I. (2011) Multivariate analyses for biomarkers hunting and validation through on-tissue bottom-up or in-source decay in MALDI-MSI: application to prostate cancer. *Anal. Bioanal. Chem.* **401**, 149–165.
- Buck A., Ly A., Balluff B. *et al.* (2015) High-resolution MALDI-FT-ICR MS imaging for the analysis of metabolites from formalin-fixed, paraffin-embedded clinical tissue samples. *J. Pathol.* **237**, 123–132.
- Caprioli R. M., Farmer T. B. and Gile J. (1997) Molecular imaging of biological samples: localization of peptides and proteins using MALDI-TOF MS. *Anal. Chem.* **69**, 4751–4760.
- Carlred L., Michno W., Kaya I., Sjövall P., Syvanen S. and Hanrieder J. (2016) Probing amyloid-beta pathology in transgenic Alzheimer's disease (tgArcSwe) mice using MALDI imaging mass spectrometry. *J. Neurochem.* **138**, 469–478.
- Chaurand P., Schwartz S. A., Billheimer D., Xu B. J., Crecelius A. and Caprioli R. M. (2004) Integrating histology and imaging mass spectrometry. *Anal. Chem.* **76**, 1145–1155.
- Chen R., Jiang X., Conaway M. C., Mohtashemi I., Hui L., Viner R. and Li L. (2010) Mass spectral analysis of neuropeptide expression and distribution in the nervous system of the lobster *Homarus americanus*. *J. Proteome Res.* **9**, 818–832.
- Cornett D. S., Reyzer M. L., Chaurand P. and Caprioli R. M. (2007) MALDI imaging mass spectrometry: molecular snapshots of biochemical systems. *Nat. Methods* **4**, 828–833.
- De Sio G., Smith A. J., Galli M., Garancini M., Chinello C., Bono F., Pagni F. and Magni F. (2015) A MALDI-mass spectrometry imaging method applicable to different formalin-fixed paraffin-embedded human tissues. *Mol. BioSyst.* **11**, 1507–1514.
- Deininger S.-O., Ebert M. P., Fuetterer A., Gerhard M. and Roegen C. (2008) MALDI imaging combined with hierarchical clustering as a new tool for the interpretation of complex human cancers. *J. Proteome Res.* **7**, 5230–5236.

- Deutskens F., Yang J. and Caprioli R. M. (2011) High spatial resolution imaging mass spectrometry and classical histology on a single tissue section. *J. Mass Spectrom.* **46**, 568–571.
- Dilillo M., Ait-Belkacem R., Esteve C. *et al.* (2017) Ultra-high mass resolution MALDI imaging mass spectrometry of proteins and metabolites in a mouse model of glioblastoma. *Sci. Rep.* **7**, 603.
- Dreisewerd K. (2014) Recent methodological advances in MALDI mass spectrometry. *Anal. Bioanal. Chem.* **406**, 2261–2278.
- Dreisewerd K., Draude F., Kruppe S., Rohlfing A., Berkenkamp S. and Pohlentz G. (2007a) Molecular analysis of native tissue and whole oils by infrared laser mass spectrometry. *Anal. Chem.* **79**, 4514–4520.
- Dreisewerd K., Lemaire R., Pohlentz G., Salzet M., Wisztorski M., Berkenkamp S. and Fournier I. (2007b) Molecular profiling of native and matrix-coated tissue slices from rat brain by infrared and ultraviolet laser desorption/ionization orthogonal time-of-flight mass spectrometry. *Anal. Chem.* **79**, 2463–2471.
- Ellis S. R., Paine M. R. L., Eijkel G. B., Pauling J. K., Husen P., Jervelund M. W., Hermansson M., Ejsing C. S. and Heeren R. M. A. (2018) Automated, parallel mass spectrometry imaging and structural identification of lipids. *Nat. Methods* **15**, 515–518.
- Esteve C., Jones E. A., Kell D. B., Boutin H. and McDonnell L. A. (2017) Mass spectrometry imaging shows major derangements in neurogranin and in purine metabolism in the triple-knockout 3xTg Alzheimer mouse model. *Biochem. Biophys. Acta.* **1865**, 747–754.
- Evans C. L., Potma E. O., Puoris'haag M., Cote D., Lin C. P. and Xie X. S. (2005) Chemical imaging of tissue in vivo with video-rate coherent anti-Stokes Raman scattering microscopy. *Proc. Natl Acad. Sci. USA* **102**, 16807–16812.
- Falsh M., Skold K., Norrman M., Svensson M., Fenyo D. and Andren P. E. (2006) SwePep, a database designed for endogenous peptides and mass spectrometry. *Mol. Cell Proteomics* **5**, 998–1005.
- Falsh M., Savitski M. M., Nielsen M. L., Kjeldsen F., Andren P. E. and Zubarev R. A. (2007a) SwedCAD, a database of annotated high-mass accuracy MS/MS spectra of tryptic peptides. *J. Proteome Res.* **6**, 4063–4067.
- Falsh M., Skold K., Svensson M., Nilsson A., Fenyo D. and Andren P. E. (2007b) Neuropeptidomics strategies for specific and sensitive identification of endogenous peptides. *Mol. Cell Proteomics* **6**, 1188–1197.
- Feider C. L., Elizondo N. and Eberlin L. S. (2016) Ambient ionization and FAIMS mass spectrometry for enhanced imaging of multiply charged molecular ions in biological tissues. *Anal. Chem.* **88**, 11533–11541.
- Fenn J. B., Mann M., Meng C. K., Wong S. F. and Whitehouse C. M. (1989) Electrospray ionization for mass-spectrometry of large biomolecules. *Science* **246**, 64–71.
- Fletcher J. S., Vickerman J. C. and Winograd N. (2011) Label free biochemical 2D and 3D imaging using secondary ion mass spectrometry. *Curr. Opin. Chem. Biol.* **15**, 733–740.
- Fonville J. M., Carter C., Cloarec O., Nicholson J. K., Lindon J. C., Bunch J. and Holmes E. (2012) Robust data processing and normalization strategy for MALDI mass spectrometric imaging. *Anal. Chem.* **84**, 1310–1319.
- Fülöp A., Sannour D. A., Erich K., von Gerichten J., van Hoogevest P., Sandhoff R. and Hopf C. (2016) Molecular imaging of brain localization of liposomes in mice using MALDI mass spectrometry. *Sci. Rep.* **6**, 33791.
- Gibb S. and Strimmer K. (2012) MALDIquant: a versatile R package for the analysis of mass spectrometry data. *Bioinformatics* **28**, 2270–2271.
- Gomes I., Sierra S. and Devi L. A. (2016) Detection of receptor heteromerization using in situ proximity ligation assay. *Curr. Protoc. Pharmacol.* **75**, 2.16.11–2.16.31.
- Goodwin R. J. A., Dungworth J. C., Cobb S. R. and Pitt A. R. (2008) Time-dependent evolution of tissue markers by MALDI-MS imaging. *Proteomics* **8**, 3801–3808.
- Goodwin R. J. A., Lang A. M., Allingham H., Boren M. and Pitt A. R. (2010) Stopping the clock on proteomic degradation by heat treatment at the point of tissue excision. *Proteomics* **10**, 1751–1761.
- Goodwin R. J., Mackay C. L., Nilsson A., Harrison D. J., Farde L., Andren P. E. and Iverson S. L. (2011) Qualitative and quantitative MALDI imaging of the positron emission tomography ligands raclopride (a D2 dopamine antagonist) and SCH 23390 (a D1 dopamine antagonist) in rat brain tissue sections using a solvent-free dry matrix application method. *Anal. Chem.* **83**, 9694–9701.
- Goodwin R. J., Nilsson A., Mackay C. L., Swales J. G., Johansson M. K., Billger M., Andren P. E. and Iverson S. L. (2016) Exemplifying the screening power of mass spectrometry imaging over label-based technologies for simultaneous monitoring of drug and metabolite distributions in tissue sections. *J. Biomol. Screen.* **21**, 187–193.
- Gorzolka K. and Walch A. (2014) MALDI mass spectrometry imaging of formalin-fixed paraffin-embedded tissues in clinical research. *Histol. Histopathol.* **29**, 1365–1376.
- Graham D. J. and Castner D. G. (2012) Multivariate analysis ofToF-SIMS data from multicomponent systems: the why, when, and how. *Biointerphases* **7**, 49.
- Groseclose M. R., Andersson M., Hardesty W. M. and Caprioli R. M. (2007) Identification of proteins directly from tissue: in situ tryptic digestions coupled with imaging mass spectrometry. *J. Mass Spectrom.* **42**, 254–262.
- Gustafsson J. O., Oehler M. K., McColl S. R. and Hoffmann P. (2010) Citric acid antigen retrieval (CAAR) for tryptic peptide imaging directly on archived formalin-fixed paraffin-embedded tissue. *J. Proteome Res.* **9**, 4315–4328.
- Hankin J. A., Barkley R. M. and Murphy R. C. (2007) Sublimation as a method of matrix application for mass spectrometric imaging. *J. Am. Soc. Mass Spectrom.* **18**, 1646–1652.
- Hanrieder J., Ljungdahl A., Falsh M., Mammo S. E., Bergquist J. and Andersson M. (2011) L-DOPA-induced dyskinesia is associated with regional increase of striatal dynorphin peptides as elucidated by imaging mass spectrometry. *Mol. Cell Proteomics* **10**, M111.009308.
- Hanrieder J., Ekegren T., Andersson M. and Bergquist J. (2012a) MALDI imaging mass spectrometry of human post mortem spinal cord in amyotrophic lateral sclerosis. *J. Neurochem.* **124**, 695–707.
- Hanrieder J., Ljungdahl A. and Andersson M. (2012b) MALDI imaging mass spectrometry of neuropeptides in Parkinson's disease. *J. Vis. Exp.* **2012** (60), pii: 3445. doi: 10.3791/3445.
- Hanrieder J., Malmberg P., Lindberg O. R., Fletcher J. S. and Ewing A. G. (2013a) Time-of-flight secondary ion mass spectrometry based molecular histology of human spinal cord tissue and motor neurons. *Anal. Chem.* **85**, 8741–8748.
- Hanrieder J., Phan N. T., Kurczy M. E. and Ewing A. G. (2013b) Imaging mass spectrometry in neuroscience. *ACS Chem. Neurosci.* **4**, 666–679.
- Hanrieder J., Malmberg P. and Ewing A. G. (2015) Spatial neuroproteomics using imaging mass spectrometry. *Biochem. Biophys. Acta.* **1854**, 718–731.
- Henderson A., Fletcher J. S. and Vickerman J. C. (2009) A comparison of PCA and MAF for ToF-SIMS image interpretation. *Surf. Interface Anal.* **41**, 666–674.
- Hishimoto A., Nomaru H., Ye K. *et al.* (2016) Molecular histochemistry identifies peptidomic organization and reorganization along striatal projection units. *Biol. Psychiat.* **79**, 415–420.

- Hummon A. B., Amare A. and Sweedler J. V. (2006) Discovering new invertebrate neuropeptides using mass spectrometry. *Mass Spectrom. Rev.* **25**, 77–98.
- Jones E. A., Shyti R., van Zeijl R. J. M., van Heiningen S. H., Ferrari M. D., Deelder A. M., Tolner E. A., van den Maagdenberg A. M. J. M. and McDonnell L. A. (2012) Imaging mass spectrometry to visualize biomolecule distributions in mouse brain tissue following hemispheric cortical spreading depression. *J. Proteomics.* **75**, 5027–5035.
- Juan A. (2018) Hyperspectral image analysis. When space meets chemistry. *J. Chemom.* **32**, e2985.
- Jurchen J. C., Rubakhin S. S. and Sweedler J. V. (2005) MALDI-MS imaging of features smaller than the size of the laser beam. *J. Am. Soc. Mass Spectrom.* **16**, 1654–1659.
- Kakuda N., Miyasaka T., Iwasaki N., Nirasawa T., Wada-Kakuda S., Takahashi-Fujigasaki J., Murayama S., Ihara Y. and Ikegawa M. (2017) Distinct deposition of amyloid-beta species in brains with Alzheimer's disease pathology visualized with MALDI imaging mass spectrometry. *Acta Neuropathol. Commun.* **5**, 73.
- Källback P., Nilsson A., Shariatgorji M. and Andrén P. E. (2016) msIQuant – quantitation software for mass spectrometry imaging enabling fast access, visualization, and analysis of large data sets. *Anal. Chem.* **88**, 4346–4353.
- Karas M. and Hillenkamp F. (1988) Laser desorption ionization of proteins with molecular masses exceeding 10000 daltons. *Anal. Chem.* **60**, 2299–2301.
- Karlsson O., Berg A. L., Lindstrom A. K. *et al.* (2012) Neonatal exposure to the cyanobacterial toxin BMAA induces changes in protein expression and neurodegeneration in adult hippocampus. *Toxicol. Sci.* **130**, 391–404.
- Karlsson O., Bergquist J. and Andersson M. (2014) Quality measures of imaging mass spectrometry aids in revealing long-term striatal protein changes induced by neonatal exposure to the cyanobacterial toxin beta-N-methylamino-L-alanine (BMAA). *Mol. Cell Proteomics* **13**, 93–104.
- Kaya I., Brinet D., Michno W., Baskurt M., Zetterberg H., Blenow K. and Hanrieder J. (2017a) Novel trimodal MALDI imaging mass spectrometry (IMS3) at 10 µm reveals spatial lipid and peptide correlates implicated in abeta plaque pathology in Alzheimer's disease. *ACS Chem. Neurosci.* **8**, 2778–2790.
- Kaya I., Brinet D., Michno W., Syvanen S., Sehlin D., Zetterberg H., Blenow K. and Hanrieder J. (2017b) Delineating amyloid plaque associated neuronal sphingolipids in transgenic Alzheimer's disease mice (tgArcSwe) using MALDI imaging mass spectrometry. *ACS Chem. Neurosci.* **8**, 347–355.
- Kaya I., Michno W., Brinet D., Iacone Y., Zanni G., Blenow K., Zetterberg H. and Hanrieder J. (2017c) Histology-compatible MALDI mass spectrometry based imaging of neuronal lipids for subsequent immunofluorescent staining. *Anal. Chem.* **89**, 4685–4694.
- Kaya I., Zetterberg H., Blenow K. and Hanrieder J. (2018) Shedding light on the molecular pathology of amyloid plaques in transgenic Alzheimer's disease mice using multimodal MALDI imaging mass spectrometry. *ACS Chem. Neurosci.* **9**, 1802–1817.
- Kelley A. R., Perry G., Bethea C., Castellani R. J. and Bach S. B. (2016a) Molecular mapping Alzheimer's disease: MALDI imaging of formalin-fixed, paraffin-embedded human hippocampal tissue. *Open Neurol. J.* **10**, 88–98.
- Kelley A. R., Perry G., Castellani R. J. and Bach S. B. (2016b) Laser-induced in-source decay applied to the determination of amyloid-beta in Alzheimer's brains. *ACS Chem. Neurosci.* **7**, 261–268.
- Kiss A., Smith D. F., Reschke B. R., Powell M. J. and Heeren R. M. (2014) Top-down mass spectrometry imaging of intact proteins by laser ablation ESI FT-ICR MS. *Proteomics* **14**, 1283–1289.
- Klinkert I., Chughtai K., Ellis S. R. and Heeren R. M. A. (2014) Methods for full resolution data exploration and visualization for large 2D and 3D mass spectrometry imaging datasets. *Int. J. Mass Spectrom.* **362**, 40–47.
- Kompauer M., Heiles S. and Spengler B. (2017) Atmospheric pressure MALDI mass spectrometry imaging of tissues and cells at 1.4-µm lateral resolution. *Nat. Methods* **14**, 90–96.
- Kruse R. and Sweedler J. V. (2003) Spatial profiling invertebrate ganglia using MALDI MS. *J. Am. Soc. Mass Spectrom.* **14**, 752–759.
- Kvartsberg H., Duits F. H., Ingelsson M. *et al.* (2015) Cerebrospinal fluid levels of the synaptic protein neurogranin correlates with cognitive decline in prodromal Alzheimer's disease. *Alzheimers Dement.* **11**, 1180–1190.
- Landgraf R. R., Prieto Conaway M. C., Garrett T. J., Stacpoole P. W. and Yost R. A. (2009) Imaging of lipids in spinal cord using intermediate pressure matrix-assisted laser desorption-linear ion trap/Orbitrap MS. *Anal. Chem.* **81**, 8488–8495.
- Lavenant G. T., Zavalin A. I. and Caprioli R. M. (2013) Targeted multiplex imaging mass spectrometry in transmission geometry for subcellular spatial resolution. *J. Am. Soc. Mass Spectrom.* **24**, 609–614.
- Ljungdahl A., Hanrieder J., Faelth M., Bergquist J. and Andersson M. (2011) Imaging mass spectrometry reveals elevated nigral levels of dynorphin neuropeptides in L-DOPA-induced dyskinesia in rat model of Parkinson's disease. *PLoS ONE* **6**, e25653.
- Longuespee R., Fleron M., Pottier C. *et al.* (2014) Tissue proteomics for the next decade? Towards a molecular dimension in histology. *OMICS* **18**, 539–552.
- Luxembourg S. L., Mize T. H., McDonnell L. A. and Heeren R. M. (2004) High-spatial resolution mass spectrometric imaging of peptide and protein distributions on a surface. *Anal. Chem.* **76**, 5339–5344.
- Maccarrone G., Nischwitz S., Deininger S.-O., Hornung J., König F. B., Stadelmann C., Turck C. W. and Weber F. (2017) MALDI imaging mass spectrometry analysis—A new approach for protein mapping in multiple sclerosis brain lesions. *J. Chromatogr. B* **1047**, 131–140.
- Marie-France R., Jean-Pierre B., Brendan P. *et al.* (2014) Software tools of the computis European project to process mass spectrometry images. *Eur. J. Mass Spectrom.* **20**, 351–360.
- Martin-Lorenzo M., Balluff B., Sanz-Maroto A., van Zeijl R. J., Vivanco F., Alvarez-Llamas G. and McDonnell L. A. (2014) 30µm spatial resolution protein MALDI MSI: in-depth comparison of five sample preparation protocols applied to human healthy and atherosclerotic arteries. *J. Proteomics.* **108**, 465–468.
- Masyuko R., Lanni E., Sweedler J. V. and Bohn P. W. (2013) Correlated imaging – a grand challenge in chemical analysis. *Analyst* **138**, 1924–1939.
- McDonnell L. A. and Heeren R. M. A. (2007) Imaging mass spectrometry. *Mass Spectrom. Rev.* **26**, 606–643.
- McDonnell L. A., Rompp A., Balluff B., Heeren R. M., Albar J. P., Andren P. E., Corthals G. L., Walch A. and Stoeckli M. (2015) Discussion point: reporting guidelines for mass spectrometry imaging. *Anal. Bioanal. Chem.* **407**, 2035–2045.
- McDonnell L. A., Angel P. M., Lou S. and Drake R. R. (2017) Mass spectrometry imaging in cancer research: future perspectives. *Adv. Cancer Res.* **134**, 283–290.
- Meding S., Martin K., Gustafsson O. J., Eddes J. S., Hack S., Oehler M. K. and Hoffmann P. (2013) Tryptic peptide reference data sets for MALDI imaging mass spectrometry on formalin-fixed ovarian cancer tissues. *J. Proteome Res.* **12**, 308–315.
- Michno W., Kaya I., Nystrom S., Guerard L., Nilsson K. P. R., Hammarstrom P., Blenow K., Zetterberg H. and Hanrieder J. (2018) Multimodal chemical imaging of amyloid plaque

- polymorphism reveals Abeta aggregation dependent anionic lipid accumulations and metabolism. *Anal. Chem.* **90**, 8130–8138.
- Monroe E. B., Annangudi S. R., Hatcher N. G., Gutstein H. B., Rubakhin S. S. and Sweedler J. V. (2008) SIMS and MALDI MS imaging of the spinal cord. *Proteomics* **8**, 3746–3754.
- Muller L., Baldwin K., Barbacci D. C. *et al.* (2017) Laser desorption/ionization mass spectrometric imaging of endogenous lipids from rat brain tissue implanted with silver nanoparticles. *J. Am. Soc. Mass Spectrom.* **28**, 1716–1728.
- Murphy R. C., Hankin J. A., Barkley R. M. and Zemski Berry K. A. (2011) MALDI imaging of lipids after matrix sublimation/deposition. *Biochem. Biophys. Acta.* **1811**, 970–975.
- Nakanishi T., Ohtsu I., Furuta M., Ando E. and Nishimura O. (2005) Direct MS/MS analysis of proteins blotted on membranes by a matrix-assisted laser desorption/ionization-quadrupole ion trap-time-of-flight tandem mass spectrometer. *J. Proteome Res.* **4**, 743–747.
- Nilsson A., Goodwin R. J., Shariatgorji M., Vallianatou T., Webborn P. J. and Andren P. E. (2015) Mass spectrometry imaging in drug development. *Anal. Chem.* **87**, 1437–1455.
- Norris J. L. and Caprioli R. M. (2013) Analysis of tissue specimens by matrix-assisted laser desorption/ionization imaging mass spectrometry in biological and clinical research. *Chem. Rev.* **113**, 2309–2342.
- Norris J. L., Cornett D. S., Mobley J. A., Andersson M., Seeley E. H., Chaurand P. and Caprioli R. M. (2007) Processing MALDI mass spectra to improve mass spectral direct tissue analysis. *Int. J. Mass Spectrom.* **260**, 212–221.
- Northen T. R., Yanes O., Northen M. T., Marrinucci D., Uritboonthai W., Apon J., Golledge S. L., Nordstrom A. and Siuzdak G. (2007) Clathrate nanostructures for mass spectrometry. *Nature* **449**, 1033–1036.
- Parry R. M., Galhena A. S., Gamage C. M., Bennett R. V., Wang M. D. and Fernández F. M. (2013) OmniSpect: an open matlab-based tool for visualization and analysis of matrix-assisted laser desorption/ionization and desorption electrospray ionization mass spectrometry images. *J. Am. Soc. Mass Spectrom.* **24**, 646–649.
- Paschke C., Leisner A., Hester A., Maass K., Guenther S., Bouschen W. and Spengler B. (2013) Mirion—a software package for automatic processing of mass spectrometric images. *J. Am. Soc. Mass Spectrom.* **24**, 1296–1306.
- Pierson J., Svenningsson P., Caprioli R. M. and Andren P. E. (2005) Increased levels of ubiquitin in the 6-OHDA-lesioned striatum of rats. *J. Proteome Res.* **4**, 223–226.
- Pietrowska M., Gawin M., Polanska J. and Widlak P. (2016) Tissue fixed with formalin and processed without paraffin embedding is suitable for imaging of both peptides and lipids by MALDI-IMS. *Proteomics* **16**, 1670–1677.
- Piqueras Solsona S., Maeder M., Tauler R. and de Juan A. (2017) A new matching image preprocessing for image data fusion. *Chemometr. Intell. Lab. Syst.* **164**, 32–42.
- Prentice B. M., Ryan D. J., Van de Plas R., Caprioli R. M. and Spraggins J. M. (2018) Enhanced ion transmission efficiency up to m/z 24000 for MALDI protein imaging mass spectrometry. *Anal. Chem.* **90**, 5090–5099.
- Prideaux B. and Stoeckli M. (2012) Mass spectrometry imaging for drug distribution studies. *J. Proteomics* **75**, 4999–5013.
- Puolitaival S. M., Burnum K. E., Cornett D. S. and Caprioli R. M. (2008) Solvent-free matrix dry-coating for MALDI imaging of phospholipids. *J. Am. Soc. Mass Spectrom.* **19**, 882–886.
- Race A. M., Palmer A. D., Dexter A., Steven R. T., Styles I. B. and Bunch J. (2016) SpectralAnalysis: software for the masses. *Anal. Chem.* **88**, 9451–9458.
- Ráfols P., Torres S., Ramírez N., del Castillo E., Yanes O., Brezmes J. and Correig X. (2017) rMSI: an R package for MS imaging data handling and visualization. *Bioinformatics* **33**, 2427–2428.
- Rausch M. and Stoeckli M. (2000) Biomap, <https://ms-imaging.org/wp/biomap/>.
- van Remoortere A., van Zeijl R. J., van den Oever N. *et al.* (2010) MALDI imaging and profiling MS of higher mass proteins from tissue. *J. Am. Soc. Mass Spectrom.* **21**, 1922–1929.
- Robichaud G., Garrard K. P., Barry J. A. and Muddiman D. C. (2013) MSiReader: an open-source interface to view and analyze high resolving power MS imaging files on Matlab platform. *J. Am. Soc. Mass Spectrom.* **24**, 718–721.
- Rompp A., Guenther S., Schober Y., Schulz O., Takats Z., Kummer W. and Spengler B. (2010) Histology by mass spectrometry: label-free tissue characterization obtained from high-accuracy bioanalytical imaging. *Angew. Chem. Int. Ed. Engl.* **49**, 3834–3838.
- Rubakhin S. S., Greenough W. T. and Sweedler J. V. (2003) Spatial profiling with MALDI MS: distribution of neuropeptides within single neurons. *Anal. Chem.* **75**, 5374–5380.
- Rübel O., Greiner A., Cholia S., Louie K., Bethel E. W., Northen T. R. and Bowen B. P. (2013) OpenMSI: a high-performance web-based platform for mass spectrometry imaging. *Anal. Chem.* **85**, 10354–10361.
- Russo R. E., Mao X., Gonzalez J. J., Zorba V. and Yoo J. (2013) Laser ablation in analytical chemistry. *Anal. Chem.* **85**, 6162–6177.
- Schmid T., Opilik L., Blum C. and Zenobi R. (2013) Nanoscale chemical imaging using tip-enhanced Raman spectroscopy: a critical review. *Angew. Chem. Int. Ed. Engl.* **52**, 5940–5954.
- Schmidt H. D., Anderson S. M. and Pierce R. C. (2006) Stimulation of D1-like or D2 dopamine receptors in the shell, but not the core, of the nucleus accumbens reinstates cocaine-seeking behaviour in the rat. *Eur. J. Neurosci.* **23**, 219–228.
- Schwamborn K. and Caprioli R. M. (2010a) MALDI imaging mass spectrometry – painting molecular pictures. *Mol. Oncol.* **4**, 529–538.
- Schwamborn K. and Caprioli R. M. (2010b) Molecular imaging by mass spectrometry—looking beyond classical histology. *Nat. Rev. Cancer* **10**, 639–646.
- Schwamborn K., Kriegsmann M. and Weichert W. (2017) MALDI imaging mass spectrometry – from bench to bedside. *Biochem. Biophys. Acta.* **1865**, 776–783.
- Schwartz S. A., Reyzer M. L. and Caprioli R. M. (2003) Direct tissue analysis using matrix-assisted laser desorption/ionization mass spectrometry: practical aspects of sample preparation. *J. Mass Spectrom.* **38**, 699–708.
- Schwartz M., Meyer B., Wirmitzer B. and Hopf C. (2015) Standardized processing of MALDI imaging raw data for enhancement of weak analyte signals in mouse models of gastric cancer and Alzheimer's disease. *Anal. Bioanal. Chem.* **407**, 2255–2264.
- Seeley E. H. and Caprioli R. M. (2008) Molecular imaging of proteins in tissues by mass spectrometry. *Proc. Natl Acad. Sci. USA* **105**, 18126–18131.
- Seeley E. H., Oppenheimer S. R., Mi D., Chaurand P. and Caprioli R. M. (2008) Enhancement of protein sensitivity for MALDI imaging mass spectrometry after chemical treatment of tissue sections. *J. Am. Soc. Mass Spectrom.* **19**, 1069–1077.
- Shariatgorji M., Kallback P., Gustavsson L., Schintu N., Svenningsson P., Goodwin R. J. A. and Andren P. E. (2012) Controlled-pH tissue cleanup protocol for signal enhancement of small molecule drugs analyzed by MALDI-MS imaging. *Anal. Chem.* **84**, 4603–4607.
- Shariatgorji M., Nilsson A., Goodwin R. J. *et al.* (2014) Direct targeted quantitative molecular imaging of neurotransmitters in brain tissue sections. *Neuron* **84**, 697–707.

- Shimma S., Sugiura Y., Hayasaka T., Zaima N., Matsumoto M. and Setou M. (2008) Mass imaging and identification of biomolecules with MALDI-QIT-TOF-based system. *Anal. Chem.* **80**, 878–885.
- Simmons D. (2008) Improved MALDI-MS imaging performance using continuous laser rastering. *Appl. Biosyst. Tech. Note.* 1–5.
- Skold K., Svensson M., Kaplan A., Bjorkesten L., Astrom J. and Andren P. E. (2002) A neuroproteomic approach to targeting neuropeptides in the brain. *Proteomics* **2**, 447–454.
- Skold K., Svensson M., Nilsson A., Zhang X. Q., Nydahl K., Caprioli R. M., Svenningsson P. and Andren P. E. (2006) Decreased striatal levels of PEP-19 following MPTP lesion in the mouse. *J. Proteome Res.* **5**, 262–269.
- Smith B. R. and Gambhir S. S. (2017) Nanomaterials for in vivo imaging. *Chem. Rev.* **117**, 901–986.
- Spengler B. and Hubert M. (2002) Scanning microprobe matrix-assisted laser desorption ionization (SMALDI) mass spectrometry: instrumentation for sub-micrometer resolved LDI and MALDI surface analysis. *J. Am. Soc. Mass Spectrom.* **13**, 735–748.
- Spengler B., Hubert M. and Kaufmann R. (1994) MALDI ion imaging and biological ion imaging with a new scanning UV-laser microprobe. In: *Proceedings of the 42nd ASMS Conference on Mass Spectrometry and Allied Topics*, pp. 1041. Chicago, Illinois.
- Spraggins J. M. and Caprioli R. M. (2011) High-speed MALDI-TOF imaging mass spectrometry: rapid ion image acquisition and considerations for next generation instrumentation. *J. Am. Soc. Mass Spectrom.* **22**, 1022–1031.
- Spraggins J. M., Rizzo D. G., Moore J. L., Rose K. L., Hammer N. D., Skaar E. P. and Caprioli R. M. (2015) MALDI FTICR IMS of intact proteins: using mass accuracy to link protein images with proteomics data. *J. Am. Soc. Mass Spectrom.* **26**, 974–985.
- Stauber J., Lemaire R., Franck J., Bonnel D., Croix D., Day R., Wisztorski M., Fournier I. and Salzet M. (2008) MALDI imaging of formalin-fixed paraffin-embedded tissues: application to model animals of Parkinson disease for biomarker hunting. *J. Proteome Res.* **7**, 969–978.
- Stauber J., MacAleese L., Franck J. *et al.* (2010) On-tissue protein identification and imaging by MALDI-ion mobility mass spectrometry. *J. Am. Soc. Mass Spectrom.* **21**, 338–347.
- Stoeckli M., Staab D., Staufenbiel M., Wiederhold K. H. and Signor L. (2002) Molecular imaging of amyloid beta peptides in mouse brain sections using mass spectrometry. *Anal. Biochem.* **311**, 33–39.
- Stoeckli M., Staab D., Wetzl M. and Brechbuehl M. (2014) iMatrixSpray: a free and open source sample preparation device for mass spectrometric imaging. *Chimia* **68**, 146–149.
- Strupat K., Karas M. and Hillenkamp F. (1991) 2,5-dihydroxybenzoic acid: a new matrix for laser desorption—ionization mass spectrometry. *Int. J. Mass Spectrom.* **111**, 89–102.
- Svensson M., Skold K., Svenningsson P. and Andren P. E. (2003) Peptidomics-based discovery of novel neuropeptides. *J. Proteome Res.* **2**, 213–219.
- Svensson M., Skold K., Nilsson A., Falth M., Svenningsson P. and Andren P. E. (2007) Neuropeptidomics: expanding proteomics downwards. *Biochem. Soc. Trans.* **35**, 588–593.
- Taban I. M., Altelaar A. F., van der Burg Y. E., McDonnell L. A., Heeren R. M., Fuchser J. and Baykut G. (2007) Imaging of peptides in the rat brain using MALDI-FTICR mass spectrometry. *J. Am. Soc. Mass Spectrom.* **18**, 145–151.
- Takats Z., Wiseman J. M., Gologan B. and Cooks R. G. (2004) Mass spectrometry sampling under ambient conditions with desorption electrospray ionization. *Science* **306**, 471–473.
- Tanaka K., Waki H., Ido S., Akita S. and Yoshida Y. (1988) Protein and polymer analysis up to m/z 100,000 by laser ionization time-of-flight mass spectrometry. *Rapid Commun. Mass Spectrom.* **2**, 151–153.
- Tarolli J. G., Jackson L. M. and Winograd N. (2014) Improving secondary ion mass spectrometry image quality with image fusion. *J. Am. Soc. Mass Spectrom.* **25**, 2154–2162.
- Taylor J. P., Hardy J. and Fischbeck K. H. (2002) Toxic proteins in neurodegenerative disease. *Science* **296**, 1991–1995.
- Thomas A., Charbonneau J. L., Fournaise E. and Chaurand P. (2012) Sublimation of new matrix candidates for high spatial resolution imaging mass spectrometry of lipids: enhanced information in both positive and negative polarities after 1,5-diaminonaphthalene deposition. *Anal. Chem.* **84**, 2048–2054.
- Ungerstedt U. (1968) 6-Hydroxy-dopamine induced degeneration of central monoamine neurons. *Eur. J. Pharmacol.* **5**, 107.
- Urban C., Buck A., Sivek J. T., Lordick F., Lubert B., Walch A. and Aichler M. (2018) PAXgene fixation enables comprehensive metabolomic and proteomic analyses of tissue specimens by MALDI MSI. *Biochem. Biophys. Acta.* **1862**, 51–60.
- Uys J. D., Grey A. C., Wiggins A., Schwacke J. H., Schey K. L. and Kalivas P. W. (2010) Matrix-assisted laser desorption/ionization tissue profiling of secretoneurin in the nucleus accumbens shell from cocaine-sensitized rats. *J. Mass Spectrom.* **45**, 97–103.
- Van de Plas R., Yang J., Spraggins J. and Caprioli R. M. (2015) Fusion of mass spectrometry and microscopy: a multi-modality paradigm for molecular tissue mapping. *Nat. Methods* **12**, 366–372.
- Vaysse P. M., Heeren R. M. A., Porta T. and Balluff B. (2017) Mass spectrometry imaging for clinical research - latest developments, applications, and current limitations. *Analyst* **142**, 2690–2712.
- Vogel A. and Venugopalan V. (2003) Mechanisms of pulsed laser ablation of biological tissues. *Chem. Rev.* **103**, 577–644.
- Walch A., Rauser S., Deininger S. O. and Hofer H. (2008) MALDI imaging mass spectrometry for direct tissue analysis: a new frontier for molecular histology. *Histochem. Cell Biol.* **130**, 421–434.
- Walker J. M., Moises H. C., Coy D. H., Baldrighi G. and Akil H. (1982) Nonopiate effects of dynorphin and des-Tyr-dynorphin. *Science* **218**, 1136–1138.
- Wang H. Y., Liu C. B. and Wu H. W. (2011) A simple desalting method for direct MALDI mass spectrometry profiling of tissue lipids. *J. Lipid Res.* **52**, 840–849.
- Wenzel R. J., Matter U., Schultheis L. and Zenobi R. (2005) Analysis of megadalton ions using cryodetection MALDI time-of-flight mass spectrometry. *Anal. Chem.* **77**, 4329–4337.
- Wiegelmann M., Dreisewerd K. and Soltwisch J. (2016) Influence of the laser spot size, focal beam profile, and tissue type on the lipid signals obtained by MALDI-MS imaging in oversampling mode. *J. Am. Soc. Mass Spectrom.* **27**, 1952–1964.
- Xu D., Omura T., Masaki N. *et al.* (2016) Increased arachidonic acid-containing phosphatidylcholine is associated with reactive microglia and astrocytes in the spinal cord after peripheral nerve injury. *Sci. Rep.* **6**, 26427.
- Yang J. and Caprioli R. M. (2011) Matrix sublimation/recrystallization for imaging proteins by mass spectrometry at high spatial resolution. *Anal. Chem.* **83**, 5728–5734.
- Ye H., Hui L., Kellersberger K. and Li L. (2013) Mapping of neuropeptides in the crustacean stomatogastric nervous system by imaging mass spectrometry. *J. Am. Soc. Mass Spectrom.* **24**, 134–147.
- Zavalin A., Yang J., Hayden K., Vestal M. and Caprioli R. M. (2015) Tissue protein imaging at 1 μm laser spot diameter for high spatial resolution and high imaging speed using transmission geometry MALDI TOF MS. *Anal. Bioanal. Chem.* **407**, 2337–2342.